TECHNICAL REVIEW

No.24 / September 2025

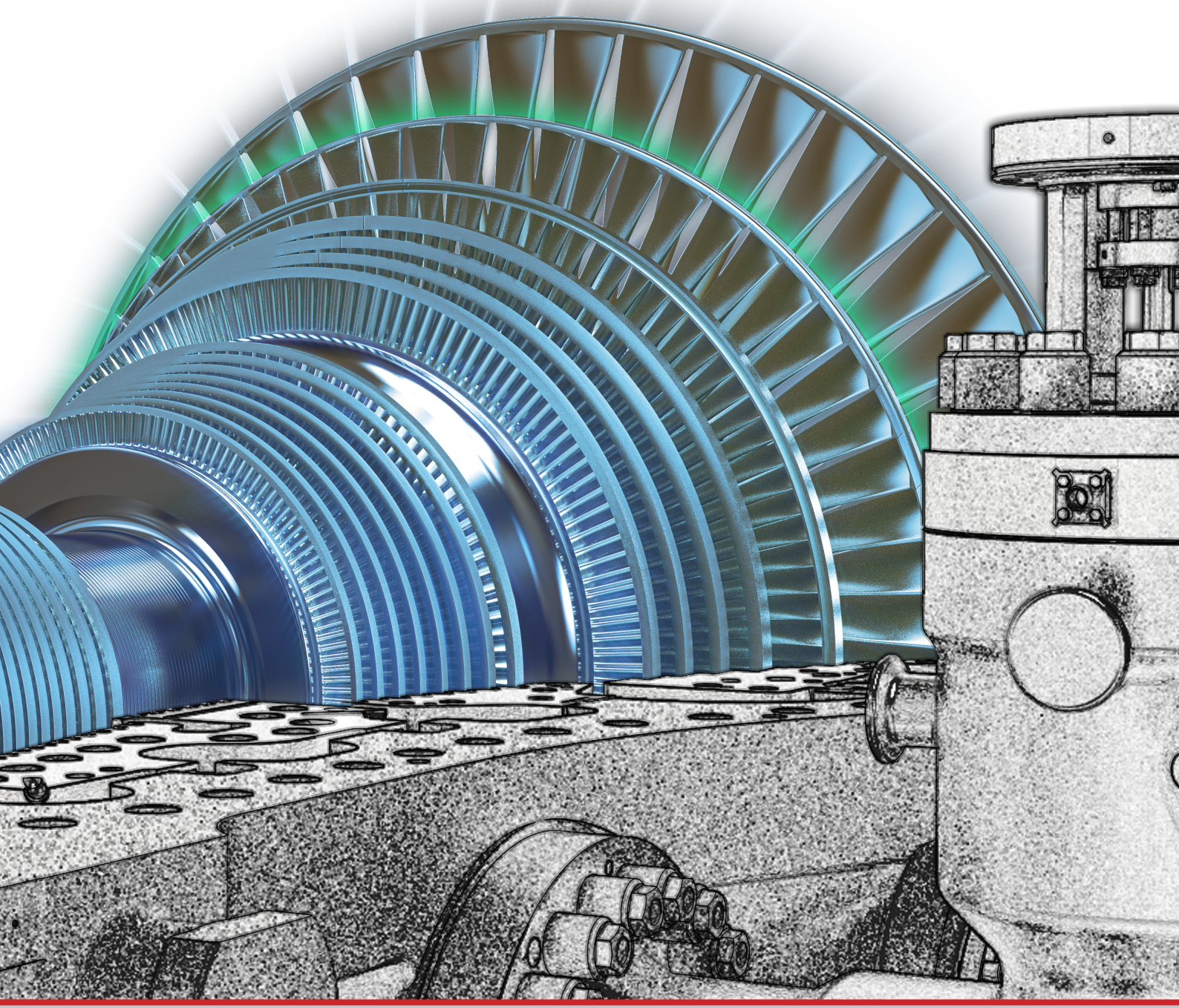

Technical Review

MAPNA GROUP
MAPNA Turbine Engineering
and Manufacturing Company

Willpower to Empower Generations

TECHNICAL REVIEW

Editorial & Production

Cover Page:
TUGA New Steam Turbine MST-50/1801

Editorial

Dear Colleagues, Partners and Professionals,

At MAPNA Turbine (TUGA), we are dedicated to proficiently developing, manufacturing, and delivering comprehensive services for gas turbines, steam turbines, and compressors essential to the energy industries across both domestic and international markets. It is in this context, and with great pleasure, that we present to you, our valued readers, a brief account of a few recent technological achievements in this edition of TUGA Technical Review.

The first article provides a concise overview of the tools developed and studies conducted for the design of TUGA's new steam turbine, the MST-50/1801. The discussed design methodology, applicable to future customized designs, ensures that blade profiles, rotors, and casings are engineered for maximum aerodynamic efficiency, enhanced resistance to fatigue and creep, and extended operational lifespan.

The second article outlines the development stages of TUGA's Steam Path Design (SPD) software utilized in the design of the steam turbine flow path. This software was also used to design the steam flow path of the MST-50/1801 steam turbine discussed in the first article. The structured and reliable methodology of this software ensures that all design parameters, from aerodynamic efficiency to mechanical stress constraints, are integrated within a unified framework.

The third article details the design and implementation of an online condition monitoring system for diesel engines. The system aims to enhance engine reliability, optimize maintenance strategies, enable early fault detection and thereby reduce the risk of severe mechanical failures by integrating real-time sensor data acquisition with advanced data analytics algorithms.

The fourth article investigates the energy-saving prospects in Computer Numerical Control (CNC) machines at TUGA through the application of advanced technologies such as real-time energy monitoring and data-driven analysis. This innovative approach not only reduces operational costs, but also supports greener manufacturing practices by minimizing idle time, enhancing energy efficiency, and decreasing machine tool wear.

A novel ceramic paste synthesized at MAPNA Turbine was studied in the final article, enabling in-situ repair methods of thermal barrier coatings (TBCs) during normal operational conditions without incurring significant downtime to mitigate the detrimental effects of elevated combustion temperatures. This improves turbine efficiency, while preserving the structural integrity of materials within the hot gas path.

Please join us in exploring a detailed account of these subjects in this issue of the Technical Review.

Respectfully,

Roohollah Jabery,

Vice President for Engineering and R&D

MAPNA Turbine Company (TUGA)

September 2025

Contents

5-15

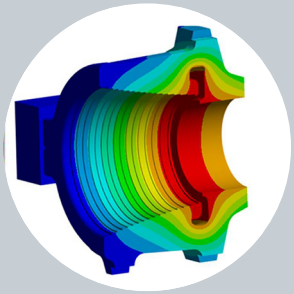

1

TUGA's MST-50/1801: Integrated Steam Turbine Design for Enhanced Performance

16-21

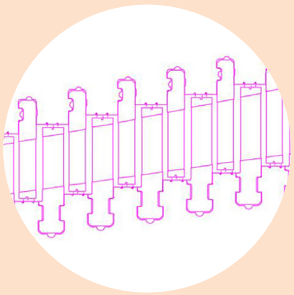

2

SPD-1D: A Precise Computational Tool for Design and Optimization of Steam Turbine Blade Path

22-27

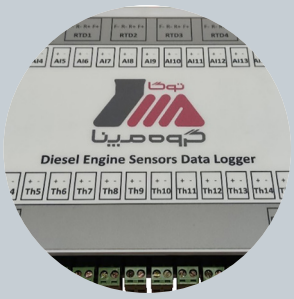

3

Online Condition Monitoring for Locomotive Diesel Engines: Improving Reliability and Maintenance Efficiency

28-35

4

Energy Management in CNC Machining Operations: Strategies for Greater Efficiency

36-43

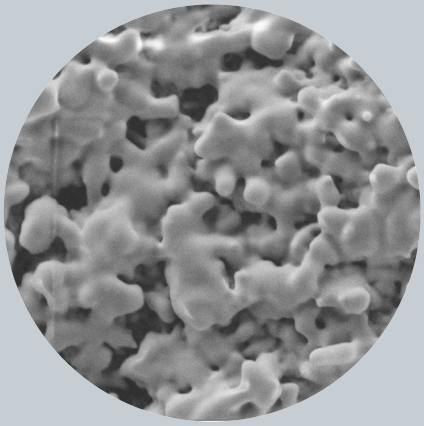

5

In-Situ Repair of Thermal Barrier Coatings: Extending Service Life Without Downtime

1

TUGA's MST-50/1801: Integrated Steam Turbine Design for Enhanced Performance

Dehestani, Pooya
Gharehbaghi, Hossein
Takdehghan, Hadi
Seifollahi, Mohammad
Ghabraei, Soheil
Ezati, Meysam
Mikaeily, Arash
Rahmaninia, Rahman
Ahmadi, Ahmad
Salehi, Ali
Sarmast, Mohammad
BaniArdalan, Mehrdad

MAPNA Turbine Engineering & Manufacturing Co. (TUGA)

Introduction

The mechanical design of steam turbines requires a multidisciplinary engineering approach to achieve efficient energy conversion, structural integrity, and reliable operation under high thermal and mechanical stresses. Central to this design are the optimization of the steam path, rotor dynamics, and casing construction, supported by advanced modeling tools such as TUGA's SPD (Steam Path Design) software[1]. These tools enable precise control of thermodynamic and mechanical parameters, ensuring that blade profiles, rotors, and casings are engineered to maximize aerodynamic performance, withstand fatigue and creep, and extend service life. Unlike studies that focus on isolated aspects of turbine design or single-stage optimization, this research presents an integrated framework that simultaneously addresses steam path, rotor, and casing optimization. This method has been applied to design of TUGA MST-50/1801 steam turbine (Figure 1) as discussed in this article. This holistic approach is particularly significant for the Iranian energy sector, where steam turbines operate under a wide range of pressures and frequent start-up/shut-down cycles, demanding enhanced durability and flexibility. Incorporating start-up and shut-down conditions, material selection, and dynamic behavior into the design process advances turbine performance and reliability tailored to Iran's industrial and power generation needs. Ultimately, this integrated design methodology lays the foundation for modern steam turbines capable of delivering efficient and reliable power generation as well as industrial process energy conversion in a rapidly evolving energy landscape.

[1] Further information on this software is provided in Article 2 of this publication.

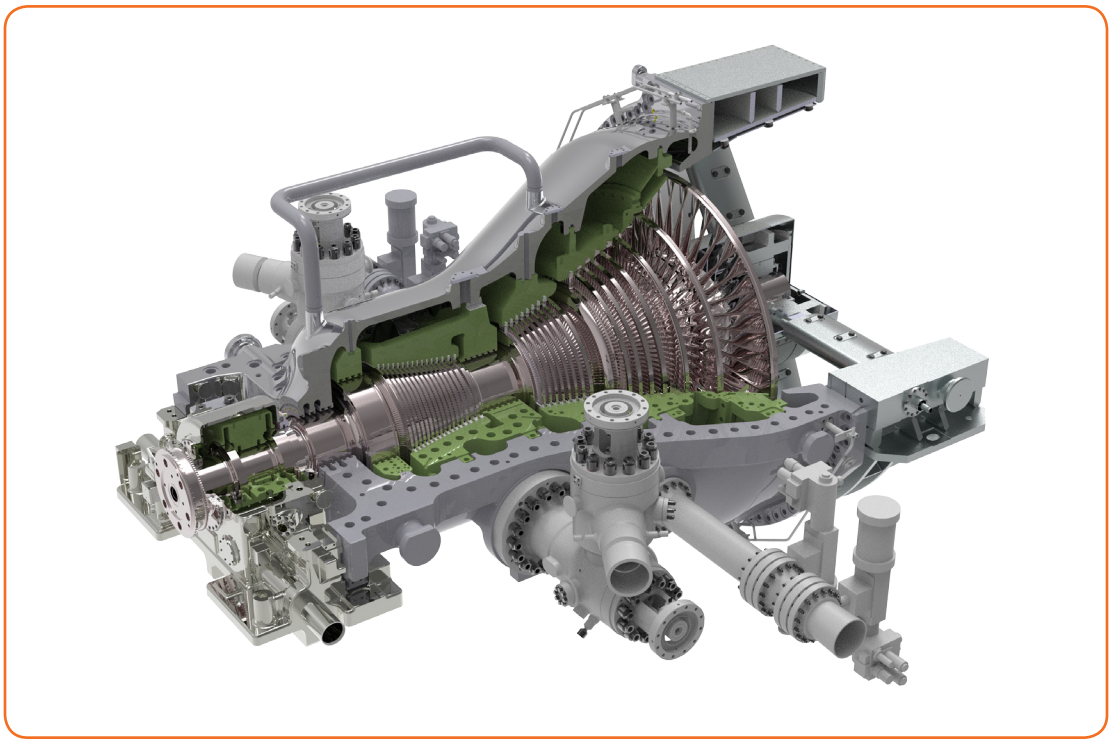

Figure 1 - TUGA's New Steam Turbine MST-50/1801

Steam Path Design

The blade path of TUGA steam turbine consists of both cylindrical and tapered/twisted blades. For cylindrical blades, the SPD software is developed to maximize thermodynamic efficiency while maintaining mechanical strength (Figure 2). This is achieved through carefully engineered blade profiles arranged in alternating rows of stationary and rotating blades. These blades are designed to withstand rotor centrifugal, aerodynamic, and thermal loads, with optimized aerodynamic profiles to minimize aerodynamic losses. The SPD's inputs include thermodynamic data from the Heat Balance Diagram (HBD), initial geometry estimation as well as aerodynamic constraints. Detailed calculations are then performed for airfoil losses (profile loss, trailing edge loss, secondary flows loss, leakage loss and moisture loss) and for the distribution of pressure, temperature, enthalpy, and steam velocity at the inlet and outlet of each row, using validated empirical correlations. Key parameters such as inlet and outlet flow angle (at hub, tip and mid-span), pitch-to-chord ratio, flow coefficient, load coefficient and reaction number are controlled within optimal design ranges. Blade section dimensions (airfoil, root, and shroud) are standardized and available in the software's library. The software computes stresses at the root and airfoil of rotating and stationary blades, claws, and connections, comparing them with allowable static and dynamic stresses. Accordingly, the allowable creep rupture strength is considered temperature dependent. The SPD also supports material selection, blade size optimization, and blade-to-rotor locking mechanisms. Furthermore, it includes special root parameter selection that reduces fatigue stress and applies blade mass reduction techniques to decrease screw connection stresses. At the end, the SPD generates blade drawing and G-code for blade manufacturing. For low-pressure stages, a set of predesigned standard blades is used.

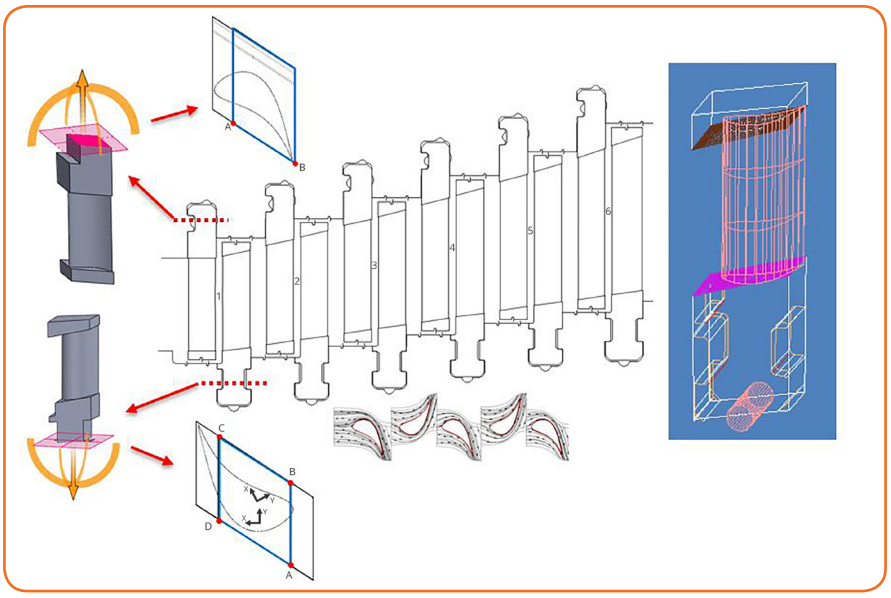

Figure 2 - Schematic for steam path design procedure by SPD

Rotor Design

The rotor is designed to resist high centrifugal loads and accommodate bending moments caused by steam-induced aerodynamic loads, temperature gradients and shaft weight. In this regard, rotor dynamic and creep-fatigue analyses are carried out to ensure the rotor's reliability and endurance. Accordingly, high-alloy steels are chosen for their strength, ductility and toughness.

■ Rotor Dynamics

Rotor dynamics is critical for turbine reliability, focusing on the behavior of the high-speed rotating shafts. The rotor is subjected to dynamic forces including axial thrust, radial loads, and unbalance-induced vibrations. Design strategies emphasize rotor balancing, optimal bearing span selection, and stiffness tuning to avoid resonance near critical speeds. Stability is enhanced by minimizing shaft deflections and controlling natural frequencies, preventing excessive vibration that could lead to fatigue failure.

A case study on the MST-50/1801 steam turbine rotor exemplifies this approach. A reduced-order model of the rotor train was developed to analyze both lateral (bending) and torsional vibrations as shown in Figure 3. Critical speeds and damping ratios for each vibration mode were calculated. To enhance operational safety, the rotor train was modified, in particular by adding an intermediate shaft which shifted the critical frequencies away from the turbine's operating speed range. In this regard, the Campbell diagram of the shaft train is generated, as shown in Figure 4.

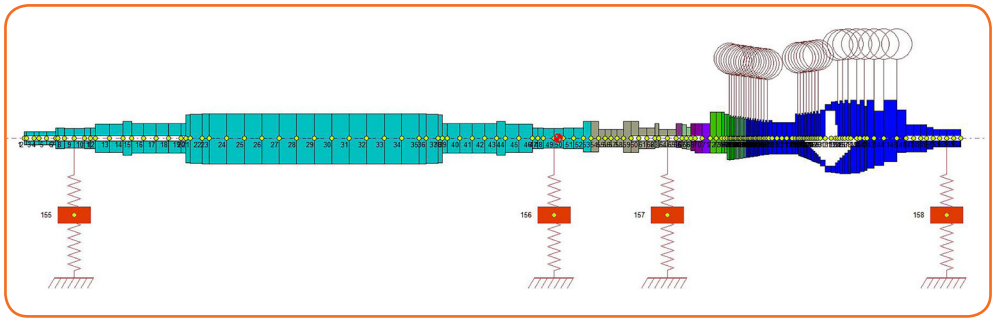

Figure 3 - Finite element model of MST-50/1801 shaft train

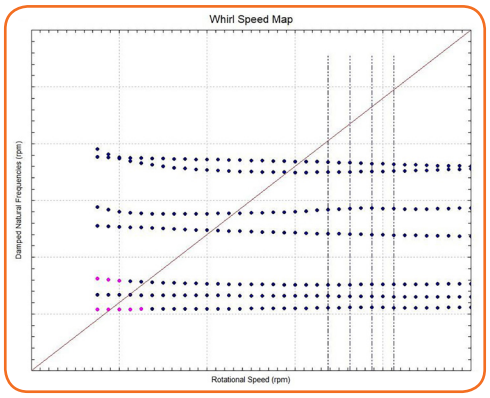

Figure 4 - Shaft train Campbell diagram

Torsional vibration analyses were also performed under generator fault scenarios. Resulting stress components were calculated and compared with proven design criteria to ensure compliance, confirming the rotor's robustness under transient conditions. The calculated first torsional mode shape, faulty torque in the shaft journal due to the out-of-phase synchronization, and shear stress contours in the extension shaft are shown in Figures 5-7, respectively.

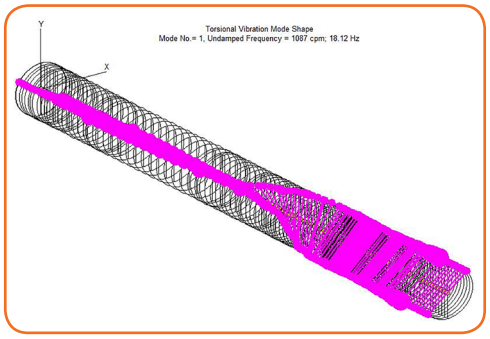

Figure 5 - Rotor train first torsional mode shape

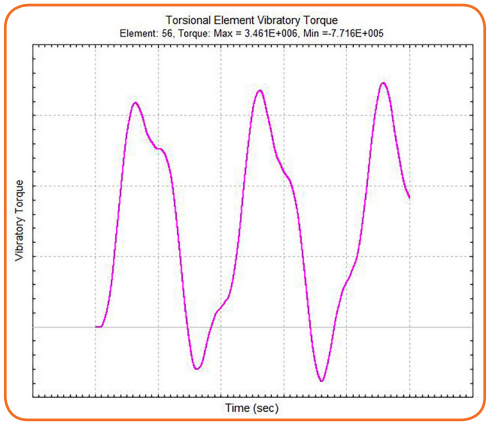

Figure 6 - Faulty torque in the shaft journal

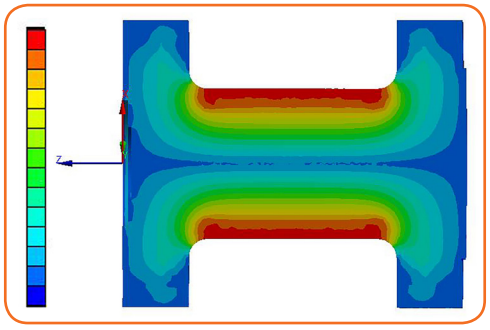

Figure 7 - Shear stress contours in the extension shaft

■ Rotor Creep-Fatigue Design

Given the high temperatures and cyclic loading conditions, fatigue strength and creep resistance are essential for long-term turbine durability. Materials are selected based on their ability to resist creep deformation and fatigue cracking over prolonged service periods, especially in high-temperature zones like rotor grooves and turbine blades. Rotor creep-fatigue design process limits stresses within safe margins and incorporates safety factors to mitigate premature failure risks.

- **Start-Up and Shut-Down**

Start-up and shut-down phases induce temperature gradients during thermal transients that cause significant stresses. The mechanical design accommodates controlled thermal expansion and contraction of rotor and casing components to prevent failure and misalignment. Bearing and casing supports are designed to allow these movements, ensuring smooth and safe operation without compromising component life. A parametric study using numerical analyses, examined over 200 states to determine the fastest safe start-up conditions, considering dwell time, temperature, load, and speed variation. The start-up curves represent the minimum safe durations; longer start-up duration increases rotor life. The design targets a minimum of 4,000 start cycles (300 cold, 700 warm, 3,000 hot cycles) and 200,000 hours of operation. Figures 8 and 9 illustrate the temperature, pressure, load, and speed during the start-up and shut-down phases.

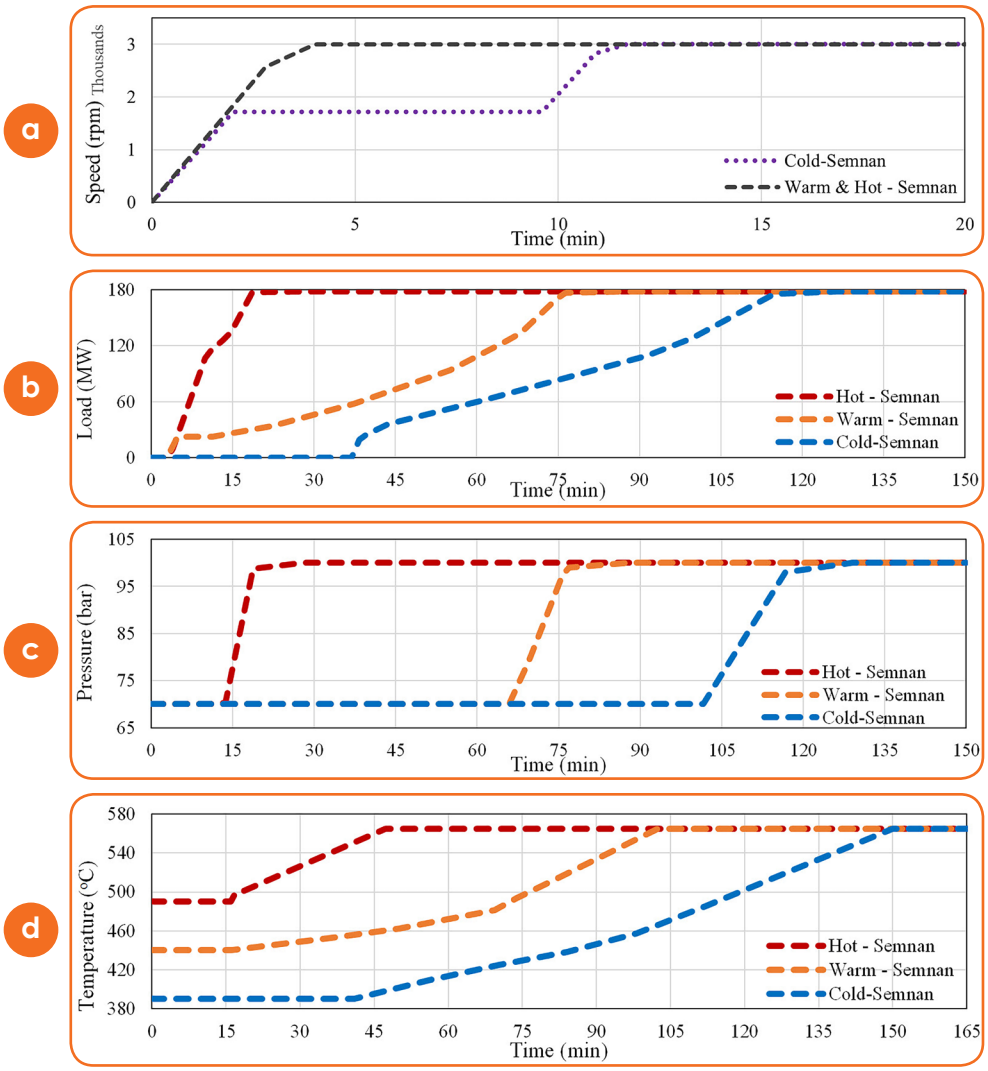

Figure 8 - (a) speed, (b) Load, (c) pressure, and (d) temperature curves over time for cold, warm, and hot startups

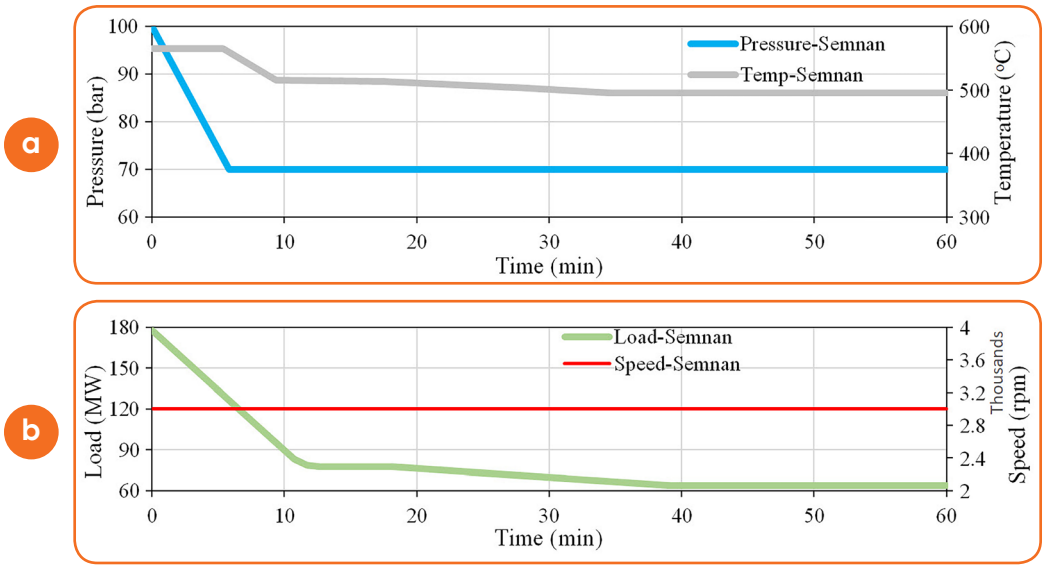

Figure 9 - (a) Temperature and pressure, (b) Load and speed curves over time for shutdown

This approach aligns with strategies to optimize start-up processes, minimize thermal stresses, and increase rotor life by controlling temperature gradients and mechanical loads during transient phases.

- **Analysis Methodology**

Modern power grids impose fluctuating demands, subjecting turbine components to thermal and mechanical stresses at elevated temperatures (e.g., 565°C). This leads to combined creep and fatigue damages, which if neglected can result in inaccurate life predictions and unexpected failures.

A finite element analysis (FEA) was employed using an axisymmetric model of a 2% Cr steel steam turbine rotor. Boundary conditions and geometrical details were modeled exactly to avoid inaccuracies caused by model simplifications. The mechanical and physical properties of the material were considered as temperature-dependent. A 4-node axisymmetric quadrilateral element with bilinear displacement and temperature fields (CAX4T) was employed to develop the finite element model of the rotor.

The analysis followed ASME Section 3-NH guidelines in three steps:

Creep Life Evaluation:

Creep life was evaluated through static stress analysis under steady-state temperature conditions. Figures 10-12 show the steady-state temperature distribution, rotor stress distribution, and creep rupture life, respectively. As high thermal stresses caused by temperature gradients are secondary and relax due to creep effects, only primary mechanical loads (e.g., centrifugal loads) were included in the creep stress analysis. The creep strain is accounted for the Low-Cycle Fatigue (LCF) analysis.

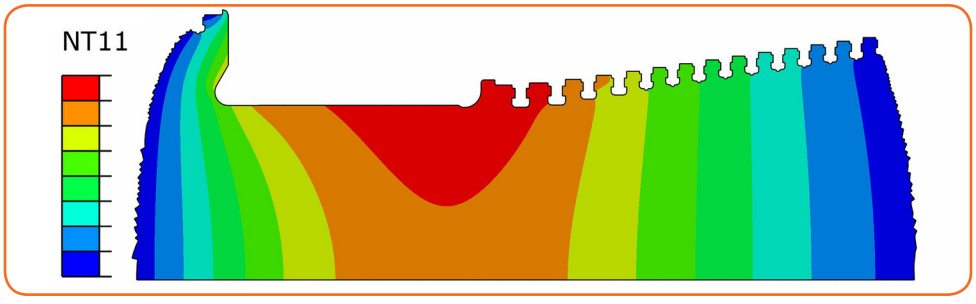

Figure 10 - Steady state temperature distribution in the rotor

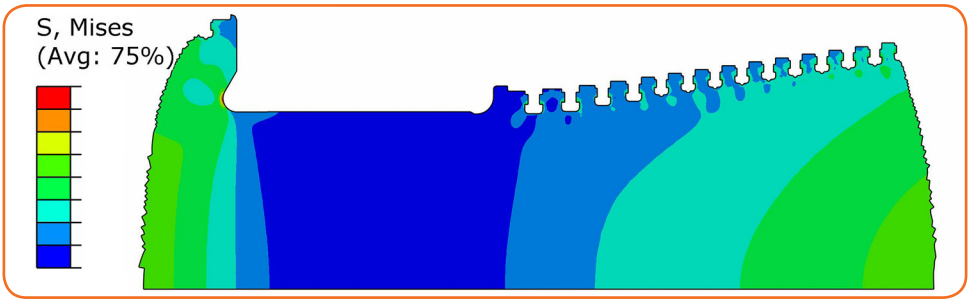

Figure 11 - Stress distribution of the rotor

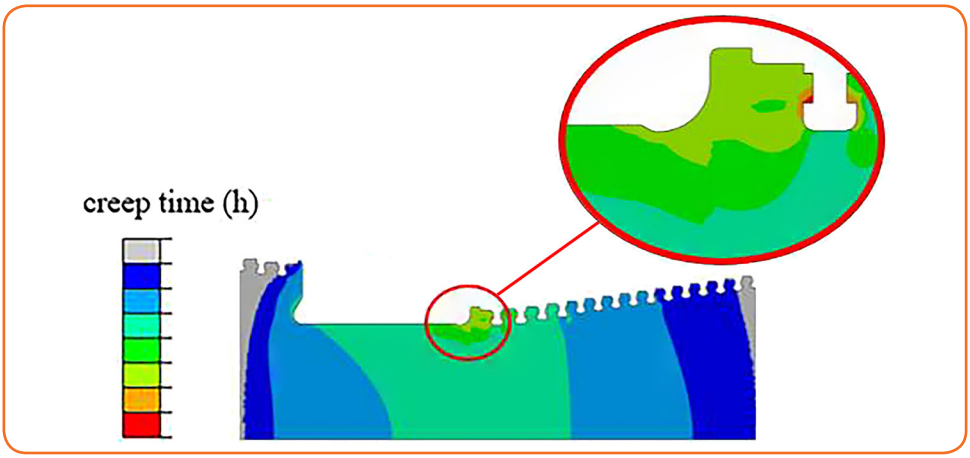

Figure 12 - Creep rupture life of the rotor

LCF evaluation:

Coupled thermal-displacement transient analyses simulated start-up and shut-down cycles. Cold, warm, and hot start-ups were simulated according to these turbine profiles. The transient analysis proceeded under normal operating conditions until the rotor attained a steady-state condition. Finally, the shutdown process was included to account for the possible cooling phase during rotor unloading. Boundary conditions incorporate variable heat transfer coefficients and steam temperature fluctuations per turbine loading recommendations. As mentioned earlier, by assuming that the whole thermal strain in steady-state conditions converts to creep strain, it is a conservative approach to add this strain to the strain range obtained in transient analyses. This combined strain is then used in the LCF evaluation. By determining the strain range at critical nodes, the LCF lifetime of each node can be estimated using the temperature and strain range data.

Creep-Fatigue interaction:

Combined damage analysis was performed per ASME Section 3-NH division T-1400.

$$\sum_{j=1}^{p}\left(\frac{n}{N_d}\right)_j + \sum_{k=1}^{q}\left(\frac{\Delta t}{T_d}\right)_k \leq D$$

In Eq. 1, D represents the creep-LCF interaction damage. N_d denotes the number of allowable design cycles for startup type j. T_d is the allowable time duration determined for the equivalent stress and the maximum temperature at the node of interest and occurring during the time interval k. n is the number of applied repetitions of startup type j. q represents the number of time intervals needed to represent the specified elevated temperature service life at the node of interest for the creep damage calculation. Δt is the duration of the time interval k. The Creep-LCF damage envelope and critical nodes are calculated and depicted in Figure 13.

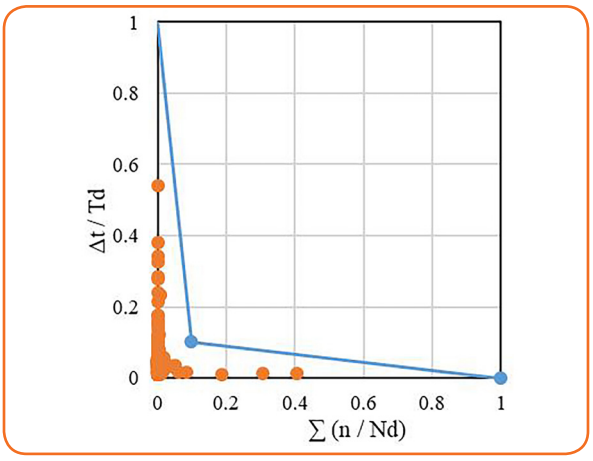

Figure 13 - Creep-LCF damage envelope and critical nodes

- **Optimization**

Optimized start-up curves are proposed to minimize creep-fatigue damage and extend rotor life. These modifications balance rapid start-up demands with reduced stress distribution, tailored to different initial temperature conditions. This comprehensive framework aids in predicting and mitigating creep-fatigue interaction, which is particularly relevant for flexible power grids with frequent cycling. It provides valuable data for maintenance strategies and component design improvements.

Casing Design

Turbine casings must endure high internal steam pressures and thermal loads, while supporting internal components. During operation, the casings should operate at minimum permissible axial and radial clearances, endure applied stresses and ensure rotor-stator alignment.

■ Inner Casing Analysis

The inner casing operates at elevated temperatures (~565°C), requiring creep-based analysis according to ASME Section 3-NH standard. Both creep and low-cycle fatigue analyses were conducted, and the results compared with creep-fatigue life diagrams.

As shown in Figure 14, a 3D model of the inner casing was analyzed symmetrically to reduce computational effort. Connecting bolts and interactions between the outer and inner casing were modeled with reasonable simplifications. The casing material, was modeled with temperature-dependent properties.

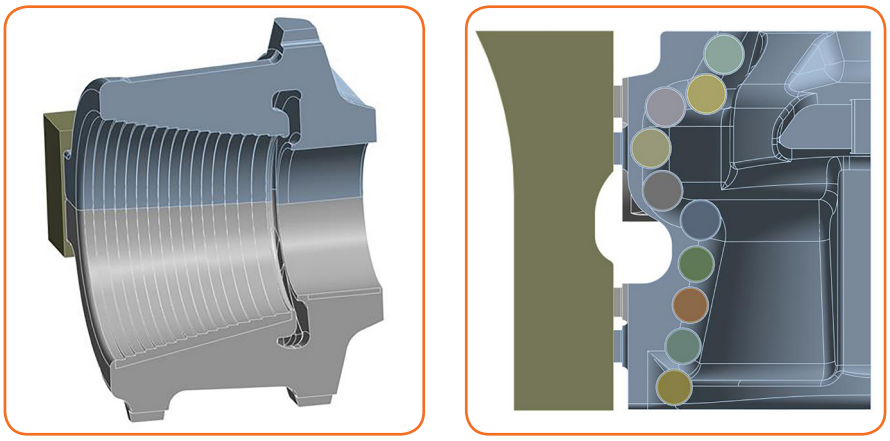

Figure 14 - 3D model of inner casing

- **Creep Analysis**

Steady-state loads (excluding thermal gradients) are applied to the model, and equivalent stresses are evaluated to estimate creep life using material-specific stress rupture-life curves. Figure 15 illustrates the temperature contour and normalized creep life of the inner casing.

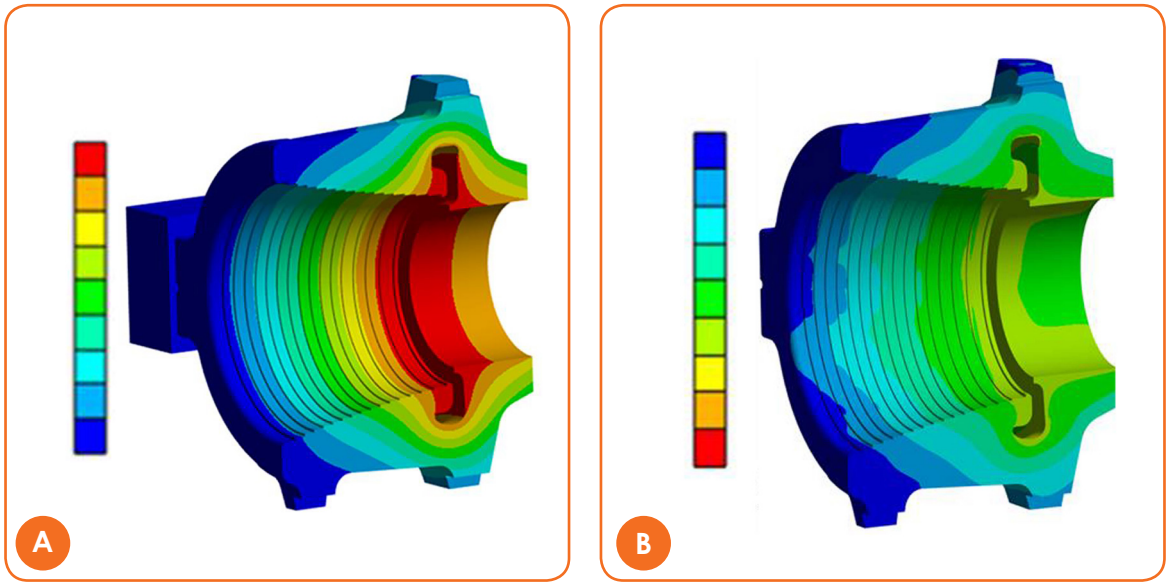

Figure 15 - A) Steady State temperature distribution B) Normalized creep life

- **Low-Cycle Fatigue Analysis**

In Low-Cycle Fatigue (LCF) analysis, a turbine start-up/shut-down cycle is modeled in ANSYS software. The analysis is performed as a transient analysis and all forces acting on the casing will be considered in this case. Then, the strain ranges at different points of the casing are calculated. Finally, the life for different strains is estimated from the strain-life diagram. In Figure 16, some evaluated LCF critical points on the casing are highlighted.

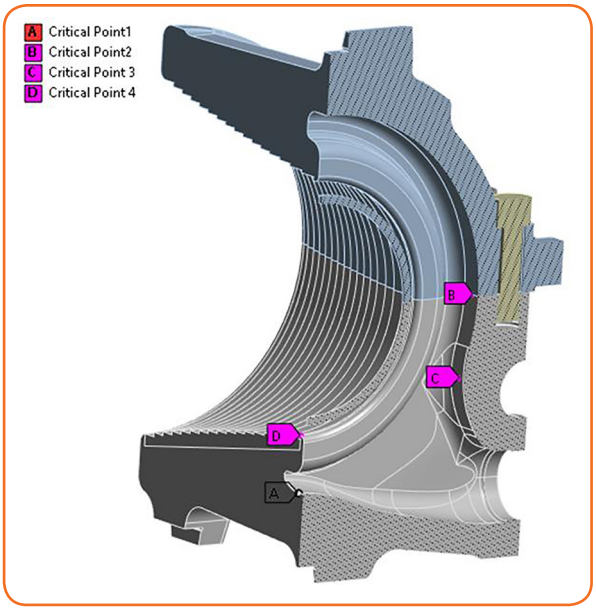

Figure 16 - Some evaluated points for Low-Cycle fatigue

- **Casing Creep-Fatigue Design**

Figure 17 shows the creep-fatigue damage envelope for inner casing material, along with corresponding damage locus of evaluated critical points at the volute and inner surface. It is observed that all critical points fell within safe regions, confirming inner casing safety.

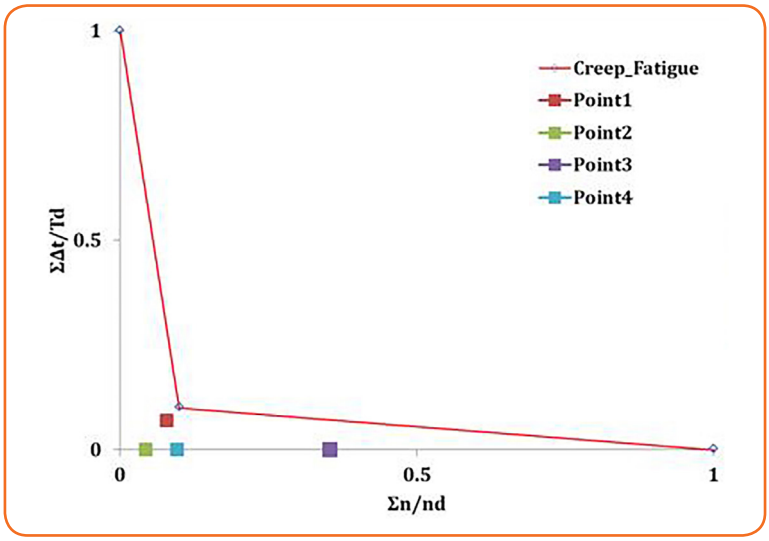

Figure 17 - Creep-Fatigue combination of inner casing

■ Outer Casing Analysis

The outer casing temperature is less than 400°C which is below the critical levels of creep mechanism. Outer casing integrity is evaluated by allowable stress values defined in ASME Section 2-Part D. The internal fluid pressure, thrust loads, weight of casings and carriers, thermal loads, and bolt preloads are considered in the FEM model. The casing material, SA-217 steel, was modeled according to ASME code. In Figure 18, steady-state temperature distribution is illustrated. Subsequently, stress analyses are performed to confirm the outer casing safety requirements under operating conditions, and the results are shown in Figure 19.

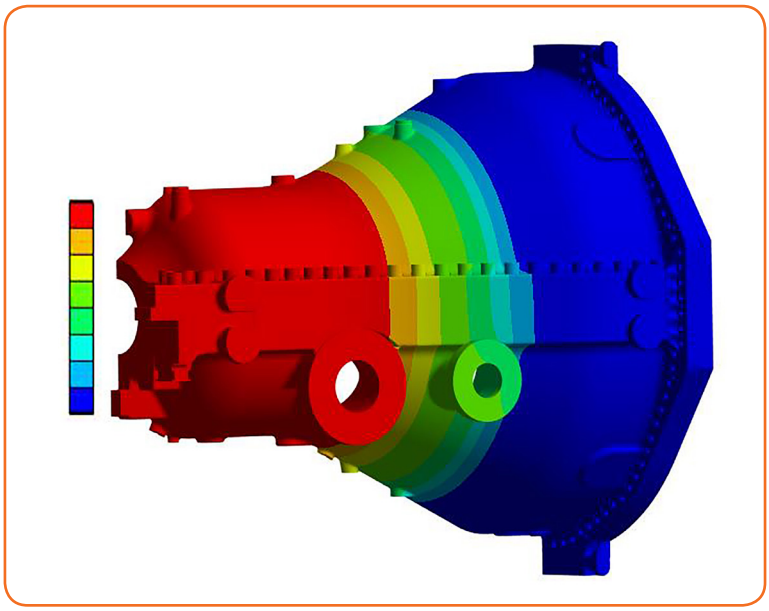

Figure 18 - steady state temperature distribution on the outer casing

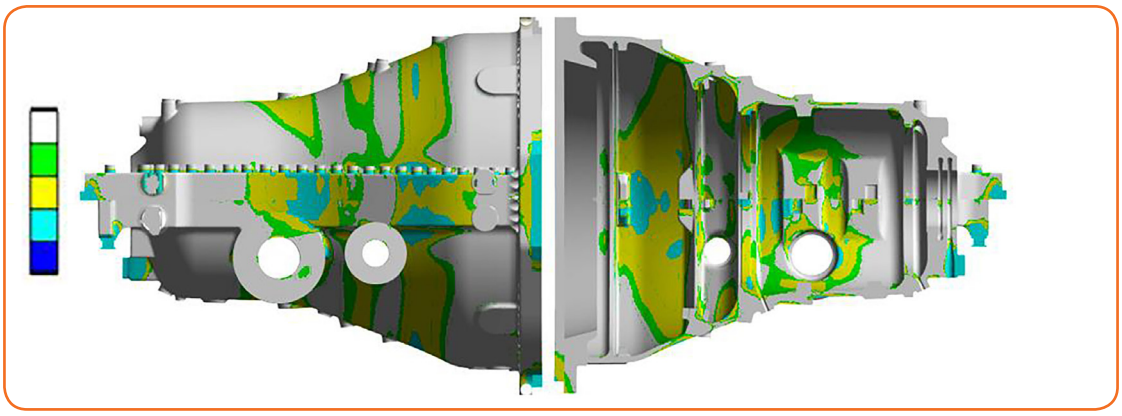

Figure 19 - Design safety factors against casing failure

Design against steam leakage from the outer casing junction is equally important and must be considered. This subject is directly associated with the bolt preloads and junction face of two upper and lower halves. The contact status depicted in Figure 20, ensures the reliability of the designed casing and its effectiveness in leakage prevention.

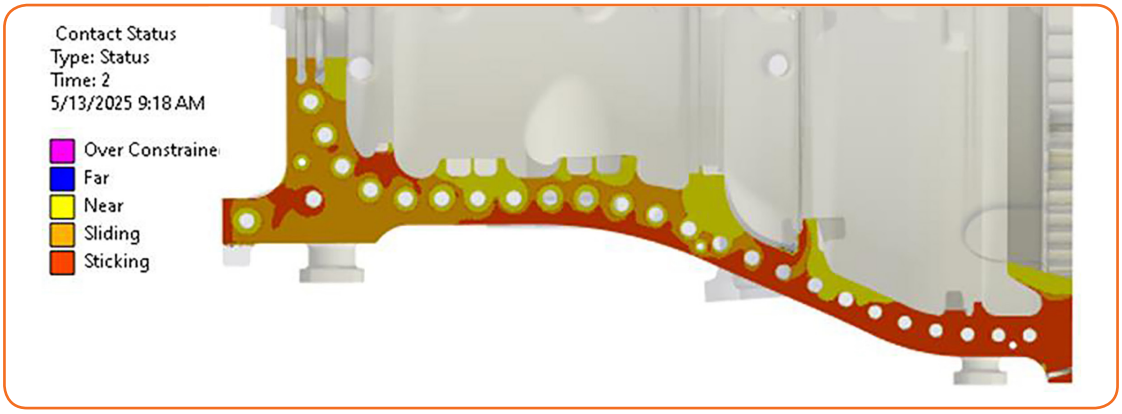

Figure 20 - Contact status in the main flange junction

Concluding Remarks

This paper provides a concise overview of the tools developed and studies conducted for the design of TUGA's new steam turbine, the MST-50/1801. To design this steam turbine, the SPD, a sophisticated tool for aerodynamic and mechanical design of steam path and turbine blading is developed. According to the SPD's steam path, the rotor and casing are designed by considerable iterations to meet the other design limitations. In this regard, rotor dynamic, creep and fatigue analyses are conducted. Rotor dynamic analysis ensures the safe operation and stability of the rotor train by calculating its critical speeds and unbalance response. A torsional analysis is carried out to ensure the shaft train's integrity in case of generator faults. Rotor and casing durability during the steam turbine life span is studied via creep-fatigue life evaluations. In this regard, a creep-fatigue life assessment is carried out by accumulating the damage on the rotor and casings due to the transient temperature gradient during startup and shutdown. The temperature dependent material properties including S-N curve, creep-rupture curve etc., have been taken into account during comprehensive life assessment. The approach to designing TUGA's new steam turbine could be implemented to develop future steam turbines according to customer demands.

2

SPD-1D: A Precise Computational Tool for Design and Optimization of Steam Turbine Blade Path

Seifollahi, Mohammad
Rahmaninia, Rahman
Takdehghan, Hadi
Gharehbaghi, Hossein
Aghaei, Mehdi

MAPNA Turbine Engineering & Manufacturing Co. (TUGA)

Introduction

The steam path of a steam turbine comprises several stages in which the expansion of the steam takes place. Each stage comprises two successive blade rows, one stationary and one rotary, converting the heat energy of the steam to the mechanical energy. For the design of a steam path, it is vital that the flow path specifications such as number of stages, dimensions and shapes of the airfoils, the sealing configurations, etc. be determined accurately. Any wrong analysis or crude approximation in the design phase may lead to an adverse effect on the performance and structural integrity of the machine. This implies the significance of accurate flow calculations in the steam path design process.

It is not feasible to use CFD as a tool for the steam path design, particularly when the steam path is composed of many stages, because it would be costly and time-consuming. Instead, it is a common practice to do 1D calculations benefiting from verified empirical models, which is largely the case with all steam turbine OEMs.

Hence, it was decided at MAPNA Turbine to acquire and expand the knowledge of 1D calculations and develop a reliable and efficient in-house computational tool to help with the design of new steam turbines. The tool is meant to calculate the flow properties of every stage of the steam path. It would be far more useful and effective if it is able to perform the required mechanical checks for the blades simultaneously and provide all the data needed for other calculations and CAD application purposes.

Given the necessity of having such a tool, its development was undertaken and successfully completed. This tool, which is called SPD-1D, is a software comprising several programs and sub-programs with a meanline code as the backbone, linked together to give a coherent design system.

SPD-1D Architecture

SPD-1D is a set of programs with a meanline code as the kernel, developed to be used as a tool for designing High-Pressure (HP) or Intermediate-Pressure (IP) blade paths comprising drum stages.

The structure outline of the code is shown schematically in Figure 1.

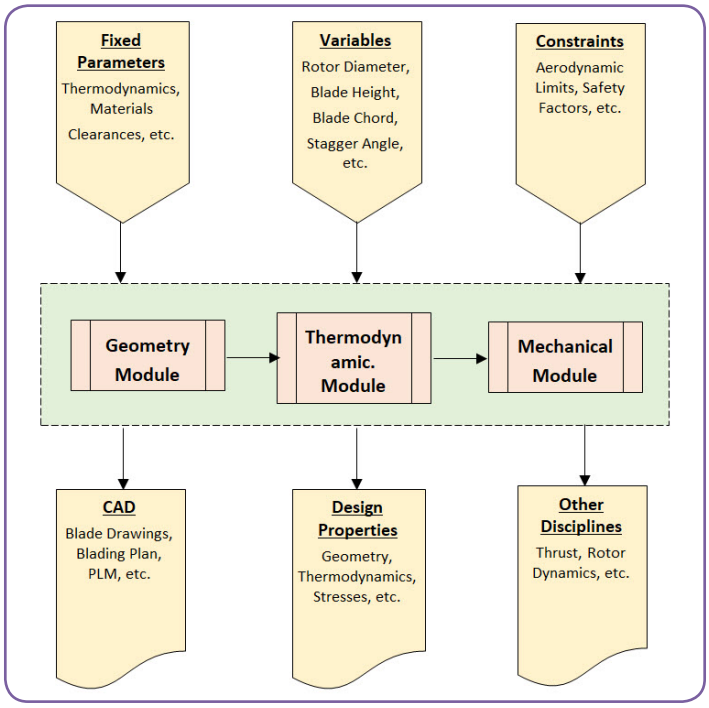

Figure 1 - SPD-1D architecture

As can be seen, the design properties of the steam path are calculated in three Steps:

- Building the geometry of the steam path
- Calculation of meanline thermodynamic properties and flow angle distributions at hub, mid and tip diameters
- Calculation of the stresses at airfoil root section, blade root, rotor claw and end-blade fixing

The resulting properties are then reviewed to check if the objectives are met. At the same time, they are checked against pre-specified constraints such as the optimum range of stage loading, flow coefficient, reaction, as well as limiting stresses.

In the current version of the code, the user should adjust the key variables such as size, stagger angle, gauging, etc. in order to reach a certain inlet pressure and temperature. However, the code reports if any design properties are deviated from the pre-specified constraints.

Although the current version of the code has not been equipped with an optimization algorithm, the user tries to specify the design variables in a way that the design properties are at their best values, while the maximum mechanical capacity of the blades is exploited. In this way, the resulting blading is thermo-economically optimized.

Geometry Module

Based on the design variables from the input file and the standard information stored in the database, the code constructs the flow path geometry. The result is a blading plan in which

the geometry of each blade including the root, airfoil and shroud is defined in both meridional and circumferential directions. The blades are arranged in the axial direction one after another based on the clearances prescribed in the input file. Grooves of both rotary and stationary blades are defined as well. Depending on the maximum relative movement, a suitable sealing configuration is considered for each blade. A meridional view of a typically designed flow path is shown in Figure 2.

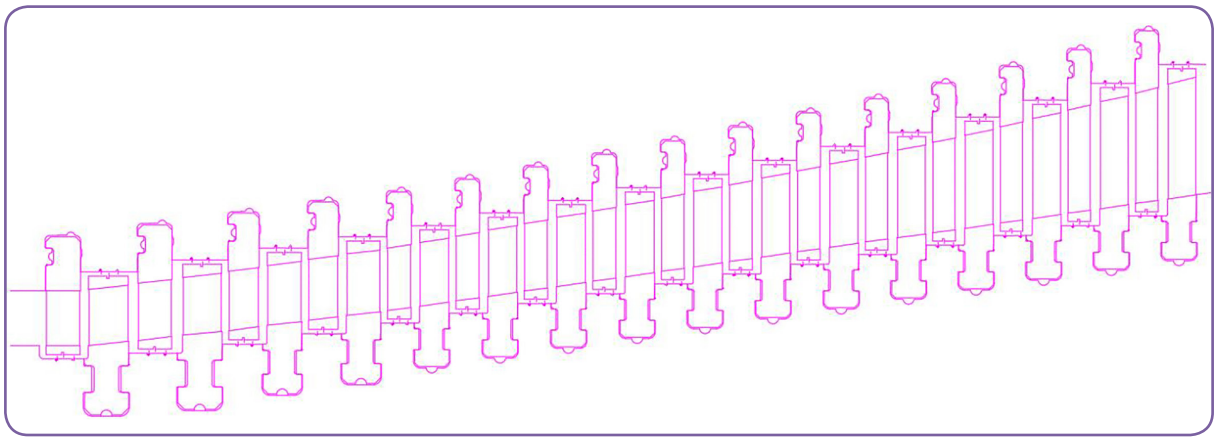

Figure 2 - Cross-sectional view of a typically-designed steam flow path

As TUGA's in-house blading technology has evolved and standardized over the years, all standard features of the blades are stored within the databases available to the software.

The following variables are read from the input file:

- Blade size (chord length)
- Blade height
- Diameters
- Stagger angle
- Axial and radial clearances
- Sealing configuration

The geometry data of the constructed blade path are used for meanline calculations in the thermodynamic module as well as for blade stress calculations.

Thermodynamic Module

Thermodynamic module is the kernel of the code developed to calculate the meanline thermodynamic properties and flow angle distributions at hub, mid and tip diameters.

The accuracy of the meanline calculation depends on the accuracy of the following correlations:

- Loss correlations
- Flow exit angle correlation

Loss coefficients are defined as the ratio of the static enthalpy loss to the relative isentropic kinetic leaving energy of the blade row. They are based on Traupel's correlation philosophy [1] adjusted to our blading technology and profile design. The accuracy of the loss models used in the code has been verified by numerous experimental investigations and CFD studies.

The following losses are considered in meanline calculations:

- Profile Loss
- Secondary Loss
- Leakage Loss
- Wetness Loss
- Additional Loss

Another set of correlations has been used to determine the exit flow angle from the stagger angle of the profile and the pitch-to-chord ratio of the flow passage. Same as the loss correlations, the accuracy of this set of correlations has been verified by numerous experimental investigations and CFD studies.

The design parameters consist of:

- Speed
- Thermodynamic boundary conditions for every blading section (design case & max. mechanical load) including the following:
  - total pressure, temperature and enthalpy at flow path inlet
  - static pressure at flow path outlet
  - mass flow rate

Thermodynamic boundary conditions are determined from thermal cycle calculations.

The first guess for some variables also comes from an in-house thermal cycle calculation code, which provides good estimates for parameters such as number of stages, blade heights and diameters.

Following each iteration, the user would check the results to see if the boundary conditions are met. Otherwise, the influencing variables would be altered until the design boundary conditions are finally reached. Special care is taken to adjust the thermodynamic/ aerodynamic parameters so as to achieve the highest efficiency. The most important parameters are as follows:

- Incidence angle
- Flow inlet angle
- Stage loading coefficient
- Flow coefficient
- Degree of Reaction

In case any of the above-mentioned parameters deviate from the pre-specified values, it is reported by the code. The user should then alter the respective input(s) to bring the concerned values within the acceptable range(s).

Verification of the meanline code has been carried out via analysis of the flow paths of several HP and IP turbine sections with drum-type blades. A good match was found between the computed results and the available field data in terms of performance and efficiency.

Mechanical Module

Following completion of the meanline design fulfilling all prescribed thermodynamic conditions, mechanical stress analysis will be performed to ensure all the stresses imposed on different components are within the acceptable ranges.

A sub-program has been developed for this purpose. This program calculates the stresses in the blade airfoil root section, blade roots, rotor claws and locking arrangements. Following data are used as input for stress calculation:

From Geometry Module:

- Full geometry of the blade including airfoil, root and shroud
- Geometry of the rotor claws
- Radial position of the blades and rotor claws

From Thermodynamic Module:

- Flow deflection over the rotor and stator blades
- Pressure drop over the rotor and stator blades
- Pressure drop over the sealing
- Steam temperature at the inlet of each blade row

To calculate the centrifugal forces acting on rotary blades, the mass and center of gravity of each part of the blade including shroud, airfoil and root are calculated. The density of the associated materials is acquired from the available databases.

Centrifugal forces impart normal stresses on the airfoil base, root neck and claw lug. Bending stresses due to centrifugal forces are calculated as well where applicable.

Bearing stresses due to centrifugal forces are calculated on the contact face of the rotary blade roots and the claw lugs.

The steam force causes bending stress at the airfoil base and the blade neck. This stress is considered a dynamic stress.

For every stress calculated at critical points of the airfoil and blade root, an allowable stress value is determined as well. This limit is a function of the yield or ultimate strength of the blade material at working temperature adjusted by respective correction factors. For high temperature zones, creep strength is considered instead of yield stress. Whether the stress is static or dynamic or a combination of the two, the corresponding stress limit is determined.

The resulting calculated stresses together with corresponding allowable ones are reported within the output file.

It is obvious that the calculated stresses must be less than the allowable ones. In case this criterion is not met, the user should interfere and alter a variable such as blade size or stagger angle to fulfill all mechanical requirements.

Another sub-program has been developed to choose the proper locking arrangement of the end-blade of each rotary blade row. The locking arrangement is either a 2-locking pin or 2-screw arrangement depending on the blade size and magnitude of the centrifugal force. Similar to the blade, the stresses within the locking pins/screws are also calculated and compared with allowable stresses. Here, the program could somehow automatically change the size of the locking arrangement or even its type to satisfy all stress and fixing requirements.

CAD Module

The CAD module has been developed to prepare the input files for CAD applications. It does not perform large calculations of its own, but rather determines further parameters using simple calculations (addition/subtraction) from the geometric data or reads in values and dimensions of standard parameters from the associated databases.

The following files are prepared by the CAD Module:

- **{Blading Plan - AUTOCAD}.scr**

  A script file containing AutoCAD commands for generating the blading plan drawing of the blade path.

- **{Blade Drawings}.scr**

  A script file containing AutoCAD commands for generating the drawings of the blades.

- **{Blading Plan - CATIA}.scr**

  A script file containing CATIA commands for generating the drawing groove plan and 3D models of the blades within 3D experience environment.

The required data for rotor-dynamics analysis as well as axial thrust calculations are also prepared.

Concluding Remarks

The SPD-1D software package serves as a comprehensive computational tool for design and analysis of steam turbine blade paths, particularly for HP and IP sections with drum-type blades. The tool applies a structured and reliable approach to the design by taking advantage of accurate 1D meanline calculations instead of time-intensive and costly CFD simulations.

The code operates through three integrated modules, ensuring all the design parameters, from aerodynamic performance to mechanical stress limits, are addressed via a unified framework. Such an approach allows for considerable time savings without undermining the design reliability.

Provision of the AutoCAD script files further enhances downstream manufacturing integration of the code, ensuring that the tool remains a valuable asset from the design phase to the manufacturing stages.

References

[1] W. Traupel, Thermische Turbomaschinen, vol. 1, 3rd ed. Berlin, Germany: *Springer-Verlag Berlin Heidelberg GmbH, 1977*.

3

Online Condition Monitoring for Locomotive Diesel Engines: Improving Reliability and Maintenance Efficiency

Emami, Arman
Izanloo, Mohammad
Deldar, Hojat

MAPNA Turbine Engineering & Manufacturing Co. (TUGA)

Introduction

In recent years, the utilization of diesel engines in various sectors such as transportation, power generation, and heavy machinery has increased significantly. Due to their high durability and satisfactory energy efficiency, diesel engines are preferred in industrial applications. However, to achieve optimal performance and maximize engine lifespan, continuous and highly accurate monitoring of operational conditions is essential. Unexpected failures can result in the disruption of critical operations and lead to substantial maintenance costs, thereby emphasizing the urgent need for an intelligent and precise approach to engine condition monitoring.

Traditional monitoring methods, which rely primarily on periodic inspections or manual evaluations, often fail to detect anomalies in a timely manner. To address these limitations, online monitoring systems have emerged as a modern solution, offering real-time tracking of key performance parameters such as temperature, pressure, vibration, and acoustic signals. By integrating real-time sensor data acquisition with advanced analytical algorithms for data interpretation, these systems can effectively identify faults at an early stage and minimize the probability of severe mechanical damage.

This paper presents the design and implementation of an online condition monitoring system for diesel engines. The primary objective is to enhance engine reliability and optimize maintenance strategies through the integration of advanced monitoring technologies.

System Architecture

An online monitoring system has been designed and implemented to monitor the condition and performance of a diesel engine and enhance its reliability. As shown in Figure 1, the block diagram of the proposed system comprises both primary locomotive components and additional equipment specifically incorporated to enable online monitoring functionality.

The system employs an RTU[1] to collect and process various input data, including signals received from the diesel engine's ECU[2], measurements from auxiliary sensors connected to a Data Logger, and geolocation data provided by a GPS[3] subsystem. The RTU transmits the aggregated data via the internet to a server, where a web-based platform has been developed to enable real-time visualization and analysis of engine performance parameters.

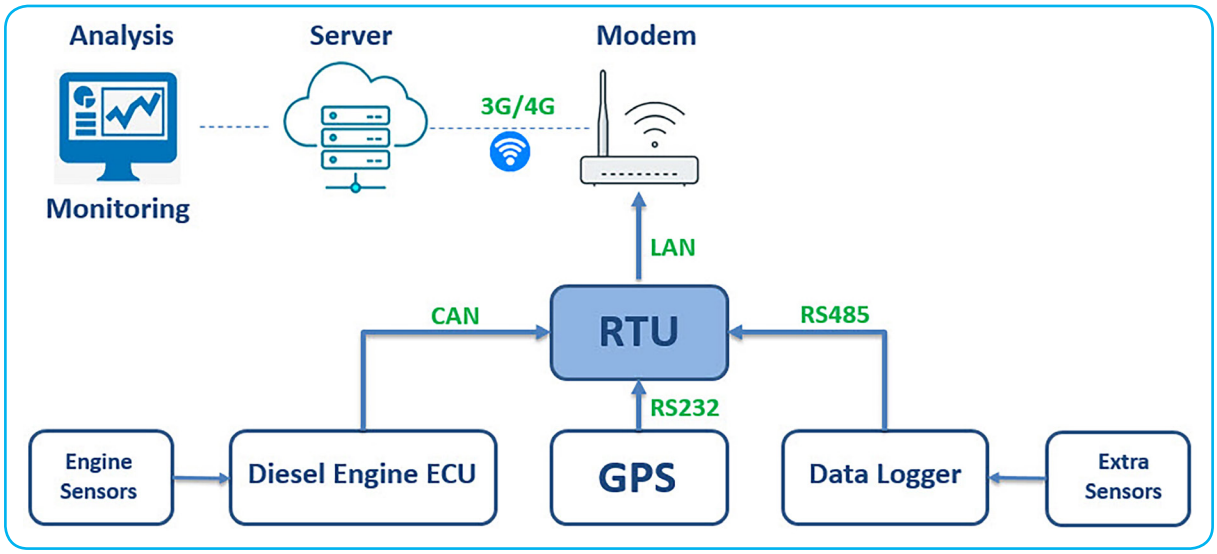

Figure 1 - Block diagram of the online diesel engine condition monitoring system

Components of the Online Monitoring System

■ RTU System

The RTU serves as the central core of the diesel engine's online monitoring system, as illustrated in Figure 2. This system includes a control board whose processor enables data exchange with both the Modbus network over an RS485 interface and CAN[4] network. The CAN port is used for reading data from the CAN network interconnecting the ECU[5] and upstream equipment, such as the PAU[6] in the locomotive or the SAM[7] in generator applications. The RS485 port is utilized for implementing the Modbus protocol and exchanging data with the Data Logger. Additionally, the control board features an RS232 port used for connecting the GPS module. Although the GPS module is housed within the RTU enclosure due to its compact form, it operates independently from a system perspective.

This control board locally stores the aggregated data on a memory card and transmits the data files to the server at scheduled intervals. Furthermore, the control board is capable of establishing a LAN[8] connection with an internet modem. The processor on this board communicates with the modem via the FTP[9] protocol over the Ethernet network, facilitating the transfer of the aggregated data files to the server.

[1] Remote Terminal Unit
[2] Electronic Control Unit
[3] Global Positioning System
[4] Controller Area Network
[5] Electronic Control Unit
[6] Power Automation Unit
[7] System Automation Module
[8] Local Area Network
[9] File Transfer Protocol

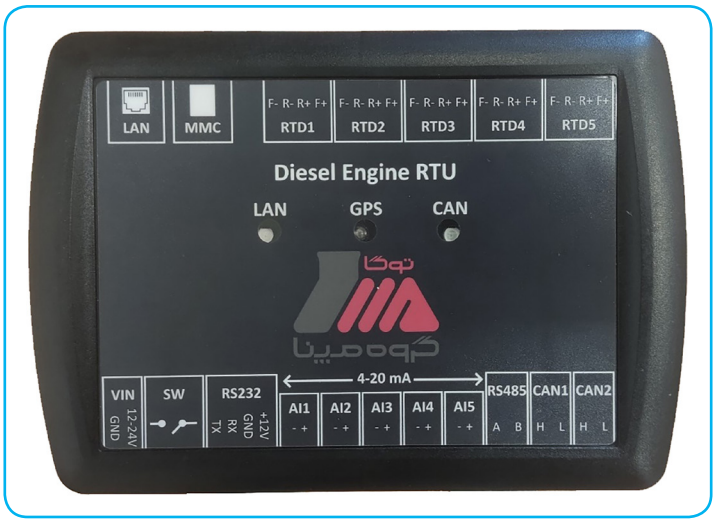

Figure 2 - Remote Terminal Unit

■ GPS Module

In applications such as railway operations, where the engine operates in a mobile environment, a GPS module continuously determines the engine's location (geographical coordinates), speed, and direction, transmitting this information to the RTU. The purpose of receiving this data is to incorporate environmental parameters such as altitude, gradient, and locomotive speed into the engine data analysis. Additionally, knowing the locomotive's position and movement direction, facilitates scheduling for engine servicing, inspections, and maintenance.

■ Auxiliary Sensors

The primary sensors of the engine are typically designed for fundamental control purposes and cannot independently provide detailed insights into the operating conditions of each component. Beyond the primary sensors, auxiliary sensors can also be integrated into the system. For Instance, by installing temperature sensors on each cylinder, temperature variations during combustion can be monitored. This enables early detection and resolution of anomalies such as incomplete combustion, imbalanced fuel distribution, or potential internal component failures.

To enhance the accuracy of diesel engine performance monitoring, various sensors can be integrated into the system depending on the type of parameter being measured. These sensors include:

- Temperature sensors for monitoring different engine subsystems such as cylinders, lubrication, air intake, and cooling system;
- Pressure sensors for measuring pressure in systems such as lubrication, fuel, and air intake;
- Level sensors for monitoring fluids such as oil, fuel, and coolant;
- Vibration sensors for detecting abnormal vibrations;
- Quality sensors for evaluating fuel, oil, or air quality;
- Gas and emission sensors for analyzing exhaust gases and controlling pollutant levels;
- Current and voltage sensors for monitoring the performance of the engine's electrical systems.

The use of these sensors improves the precision of engine condition monitoring, prevents potential damage, and enhances the overall efficiency of the system.

■ Data Logger

Another essential element of the diesel engine's online condition monitoring system is the Data Data Logger (Figure 3), designed for real-time data acquisition. This system includes an electronic board capable of connecting temperature sensors (such as RTD sensors) and sensors with 4-20mA current output. The central processor of this board samples temperature and pressure values from various sensors at specified intervals. This data can be transmitted to the RTU via the Modbus protocol over the RS485 interface. In this setup, the RTU operates as the Modbus master, while the Data Logger board functions as the Modbus slave. Therefore, at predetermined intervals, the RTU sends a request to the Data Logger to read the sensor values. In response, the Data Logger places these values into Modbus registers and sends them back to the RTU.

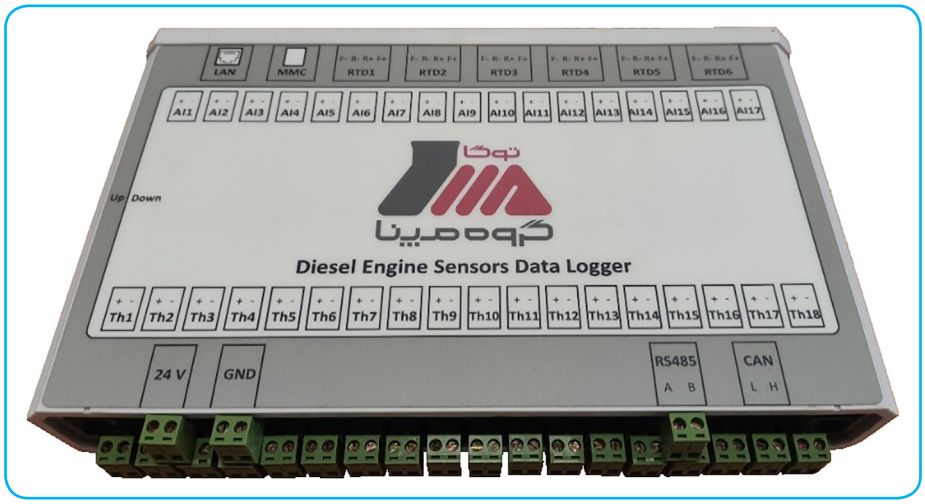

Figure 3 - Data Logger

■ Communication between the CAN Network and the ECU

Through the CAN network, sensor data is rapidly and securely transmitted to the ECU, facilitating the distribution of critical engine parameters to other subsystems. These parameters encompass:

- Temperatures of engine, coolant, and exhaust
- Pressures of oil, fuel, and intake/exhaust air
- Levels of fuel, oil, and radiator coolant

Furthermore, data related to engine rotational speed and turbocharger performance are also shared.

Furthermore, command and control data, including instructions for actuators such as fans and pumps, as well as requests from higher layers such as requested engine speed and torque, are sent to the ECU. System status information also forms an essential part of the data, including the on/off status of the engine, auxiliary systems like fans and thermostats, turbocharger, and safety systems. Finally, fault diagnosis codes for identifying potential malfunctions and performance data such as engine load, output power, fuel consumption, and combustion efficiency are provided to the ECU for performance analysis.

■ Server and Monitoring Software

The acquired data is stored on a server and made available to the user through a web-based Graphical User Interface (GUI). Users can access the monitoring panel via a web browser to visualize real-time engine data. The data is also presented in the form of time-series graphs, filterable tables, and downloadable reports.

As shown in Figure 4, the web page developed for displaying engine data connects to the database on the server, providing access to data from individual engines. By selecting the engine number and the desired data, the user can observe the corresponding changes over a selected time period.

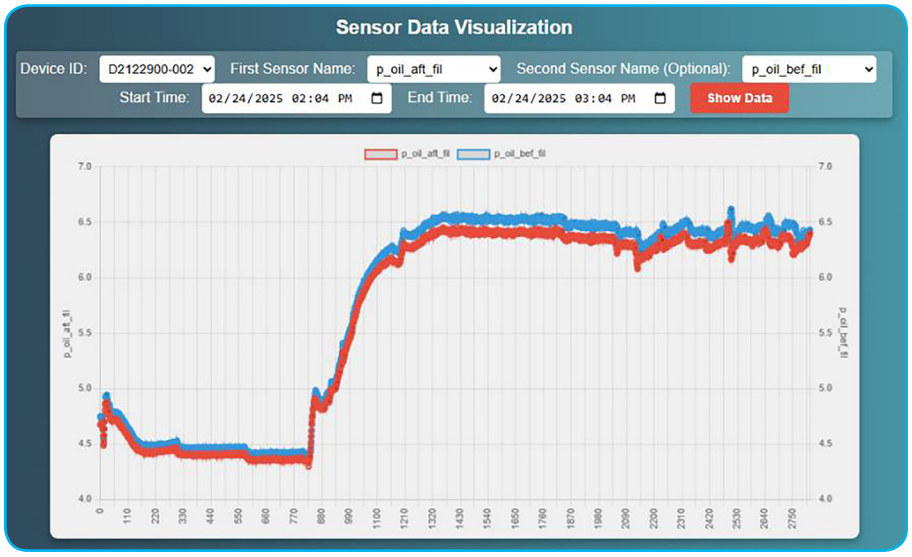

Figure 4 - Engine data displayed on the server-based web monitoring system

Figure 5 illustrates the web page designed to display the geographical location of the engine installed on the locomotive, along with the date and time.

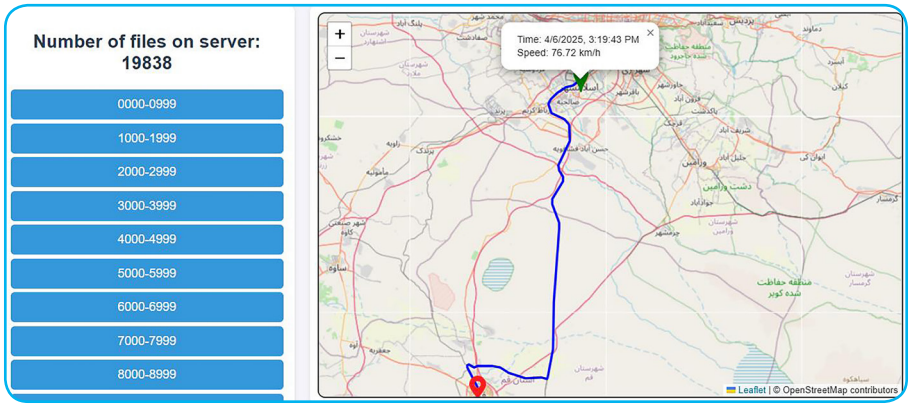

Figure 5 - Engine location displayed on the web-based system hosted on the server

Advantages and Applications of the System

The implementation of an online condition monitoring system for the diesel engine can provide numerous benefits. By enabling real-time monitoring of engine performance, this system facilitates the identification of anomalies before they lead to serious failures, thereby reducing downtime and repair costs. Additionally, utilizing online data can result in improving preventive maintenance and managerial decision-making.

In the railway transportation industry, such systems can play a vital role in enhancing productivity and reducing costs. By identifying and addressing problems prior to major failures, the engine's lifespan is extended, and operational costs are significantly reduced.

The advantages of the designed and implemented system include the following technical capabilities:

- Data storage for long-term historical analysis of engine performance.
- Threshold definitions with automatic alerts upon the detection of parameters exceeding the allowed limits.
- Real-time tracking of the location of mobile engines (such as diesel vehicles) displayed on a map.
- Integration of an increased number of installed auxiliary sensors.
- Implementation of alerting and control algorithms for response to emergency situations.

Concluding Remarks

In this paper, the design and implementation of an intelligent system for the online monitoring of diesel engines were examined. By integrating three data sources, GPS location data, additional sensors connected to a Data Logger, and technical information published on the CAN network by the engine's ECU and PAU, this system enables comprehensive, real-time monitoring of engine performance.

Through this system, users can remotely access and analyze vital engine data in real-time through a web-based platform. This capability leads to enhanced safety and reduced preventive maintenance costs. Furthermore, in mobile applications, it provides the ability to track the engine's real-time location.

The obtained results demonstrate that combining industrial and internet communication platforms, along with a suitable user interface, can form the foundation for a cost-effective, scalable, and reliable solution for monitoring engine equipment in various industries.

One of the important future aspects of this system is the potential implementation of intelligent fault diagnosis algorithms, such as AI-based methods and machine learning models. These algorithms can be implemented on the server, and by analyzing the data acquired from sensors and engine parameters, can automatically detect anomalies and potential malfunctions, sending necessary alerts. Additionally, the development of mobile applications for easier access to information will be another step in the system's development.

4

Energy Management in CNC Machining Operations: Strategies for Greater Efficiency

Safari, Soheila
Daneshmandi, Alireza
Almaszadeh, Mohammad
Vahebi, Mehrdad

MAPNA Turbine Engineering & Manufacturing Co. (TUGA)

Introduction

Energy costs and environmental problems must be properly addressed in today's competitive manufacturing ecosystem. The prevailing view is that HVAC systems, lighting, and other process-level operations are the preferable places to look for energy saving opportunities. Consequently, the energy management regulations have made no focus on metal-cutting machine tools due to the non-steady energy usage patterns of those appliances. The issue is particularly complex in Computer Numerical Control (CNC) machine tools due to the presence of sequential subsystems and extensive interactions between them. This study investigates the prospects of energy saving in the CNC machines at TUGA and the pivotal role it can play in the shop's overall energy saving strategy by applying cutting-edge technologies like real-time energy monitoring and data-driven analysis. This paradigm shift not only decreases costs but also aligns with the global push for greener manufacturing practices. Globalizing these technological achievements in terms of strategic approaches provides the potential to shift the traditional views of metal cutting sector owners toward more sustainable and efficient insights.

Overview of CNC Machines

Five-axis metal-cutting CNC machines are the most advanced type of CNC technology, utilized to manufacture complicated and precise parts in a variety of industries. A typical five-axis CNC machine comprises three linear axes (X, Y, and Z) and two rotational axes (A and B), which enable the tool to cut free-form features on the workpiece (Figure 1). Along with the numerous advantages that five-axis CNC machines provide, they necessitate accurate energy management and monitoring activities to reduce the operational expenses and increase their productivity.

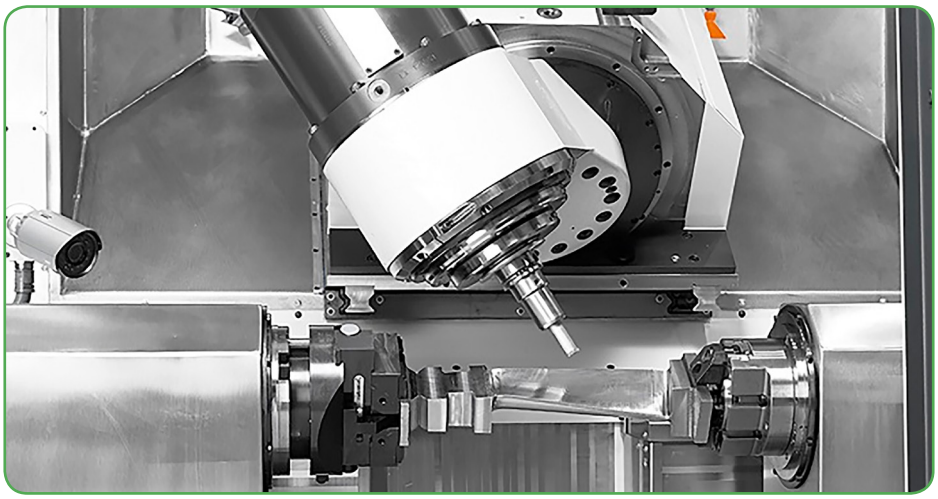

Figure 1 - Typical five-axis CNC machining of a turbine blade

Five-axis CNC machines are made up of numerous important subsystems that work together to complete machining tasks; including:

- **Main Controller**, which controls drive and axis movements. Its primary function is to regulate the motion of the system's axes using the operator's program (G-code) and parameters.
- **The Programmable Logic Controller (PLC)**, which controls machine features like safety logics and non-CNC auxiliary controls, such as tool/head changer system operations.
- **Linear motion axes**, which provide precision and controlled linear motion along X, Y, and Z axes.
- **Rotary motion axes** (namely A, B, and C axes), which provide precise and controlled linear motion around X, Y, and Z axes.
- **The spindle**, which holds and rotates the cutting tool and consumes most of the machine's energy. The spindle's speed and precision directly affect machining quality.
- **The cooling system**, which lowers the temperature of critical elements like the spindle and other important elements such as bearings.
- **The Lubrication System**, which reduces friction and wear in the motion axes and internal components.
- **Automatic Tool Changer (ATC)**, which includes the Tool Magazine and tool changing mechanism.
- **The Tailstock and Chuck**, which utilize hydraulic pressure to fix the workpiece firmly into the workpiece-carrying axes.

To follow up on the energy saving idea, all of the aforementioned subsystems should be thoroughly investigated.

Data gathering preparations

The motion control part of CNC machines is generally outfitted with advanced design that minimizes electrical energy consumption and hence has the least need for saving. On the other hand, the auxiliary sub-systems and operation conditions are prone to many uncertainties, suggesting a great potential for energy saving.

Metering graphs of input power measurement mounted on a common CNC machine tool, indicated a complex energy consumption pattern for the device. To deal with the pattern's complexity, saving options such as pre-filtering cooling liquid, resetting the chillers' start/stop temperature, altering the hydraulic system's pressure setting, and replacing inverters or soft starters on auxiliary electro pumps were investigated one by one. While some improvements in energy consumption or system operation were observed, most of these saving options were not found to be significantly cost-effective and didn't provide enough power savings. Nevertheless, other elements such as operator performance, climatic conditions, and supplemental system performance, seemed to have a more significant impact on overall energy usage.

To determine the most effective variables, a data collection process was launched, capturing all accessible data such as temperature, humidity, machining/idle time, current, voltage, and so on. Figure 2 illustrates the devices required to conduct the experimental part of the case study. The data was continuously and accurately collected to facilitate the analysis of energy consumption and machine performance. Figure 3 shows the installation of the additional metering devices by maintenance technicians on the electrical cabinet of a machine tool for the sake of data consistency. The digital temperature data logger was used for monitoring and recording temperature values at high speed over long periods. The sampling rate can be adjusted from 1 minute to 24 hours. These values are easily readable on a computer via a USB interface, which helps generate PDF reports of the recorded information. The data logger used in this project was the CEM DT-191 model, as shown in Figure 2-a. For measuring current, voltage, frequency, power factor, active and reactive power, as well as energy, a power meter was used (Figure 2-c). This metering device was embedded in a network-based live data sending package (Figure 2-d) to log all metering data in a central PC. To ensure this package's accuracy, an external power analyzer was used (Figure 2-b). The data from the power analyzer was compared with the data collected from the data loggers to verify that the results were accurate and reliable.

a) Temperature data logger

b) Standalone power analysis device

c) Installable metering device

d) Customized network-based metering assembly

e) Real-world CNC machine tool

Figure 2 - Main elements of energy-monitoring case study

Figure 3 - Installation of power meter and data logger

At the beginning of the process, the operation-level data was gathered using a handheld device (Figure 4) carried by the machine operator, but this method resulted in inaccuracies, causing considerable disparities between the recorded and real values.

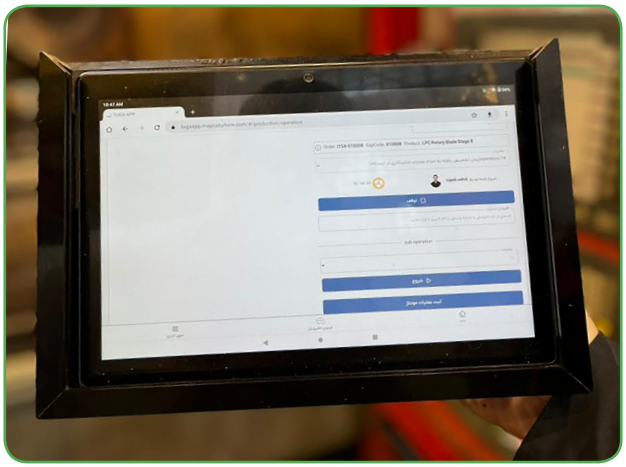

Figure 4 - Data registration with handheld device

To capture real-time data without human intervention, sophisticated PLC coding was applied to the machine's control system (Figure 5). After examining and detecting the machine's various working modes, two programs were created: one called AUTO to register productive machining operations, and another called IDLE to register non-productive machining operations. These programs automatically and more accurately recorded the Machine's productive and non-productive operation hours in terms of time vs energy in both AUTO and IDLE states. This solution prepared real-time and reliable data even for long-term and continuous production processes, which is necessary for the data analysis stage.

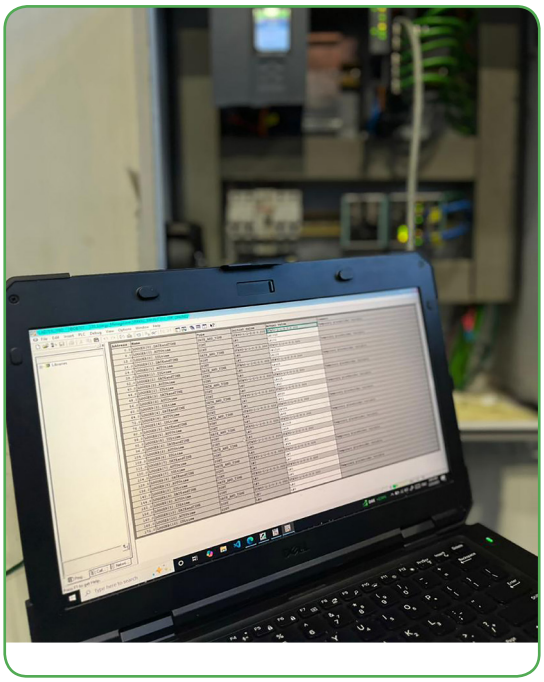

Figure 5 - PLC program and transferring industrial PC

Initial data analysis indicated two essential early-stage results: first, humidity has no major impact on energy usage, and second, the daily energy consumption of a typical CNC machine tool is a combination of four distinct dominating patterns.

Energy usage modelling

After a six-month continuous monitoring of non-productive electrical energy consumption on a typical 5-axis CNC machine tool, some strong evidence about a considerable potential for power savings through controlling the process of machine tool operation was obtained. A data analysis indicated an important correlation between total energy consumption and idle time, or non-productive hours.

■ Pattern recognition of energy usage

According to electrical energy consumption metering timelines, during each working day, there are four distinct recurring patterns, which are outlined below:

- **Machining state** refers to the situation when the machine is actively performing the material removal process on the workpiece. During this time, the Energy consumption of the machine includes both the Energy used by auxiliary equipment and the Energy consumed by the machining process itself (Figure 3-a).
- **Idle state** refers to the period when all main and auxiliary systems are powered on, but no machining activity is taking place. This state is frequently caused by workpiece setup, operation quality checks, operator rest, maintenance diagnostics, etc. (Figure 3-b).
- **Drive-Off state** (Figure 3-c) in a five-axis CNC machine occurs under the following conditions:
  - When the machine is powered on, but the drives are still off.
  - When the machine is in an emergency state.
- **Machine-off state** is the state that the power supply to the control panel is turned off, resulting in zero energy consumption.

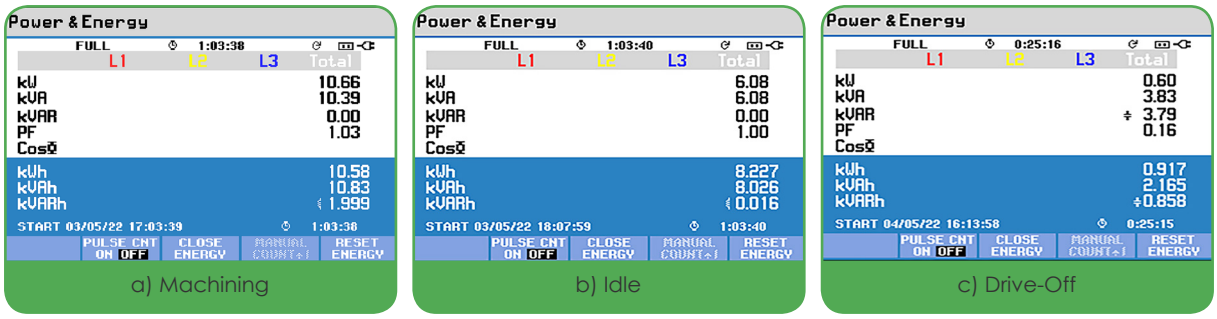

Figure 6 - Metering sheets in different states

Figure 4 indicates that, despite the common belief, the machine tool's energy consumption in the Idle state is nearly identical to that in the machining state. This fact, in general, is related to the active standing of the direct drive motion control system while the machine appears to be relaxed and in a low energy mode. Accordingly, the data study revealed that implementing an "Idle-to-Drive-Off transition policy", which includes promptly turning machines off during unproductive times, significantly reduced energy consumption by machine tools. Besides the reduction in energy consumption and costs, this also increases productivity and slows machine tool degradation.

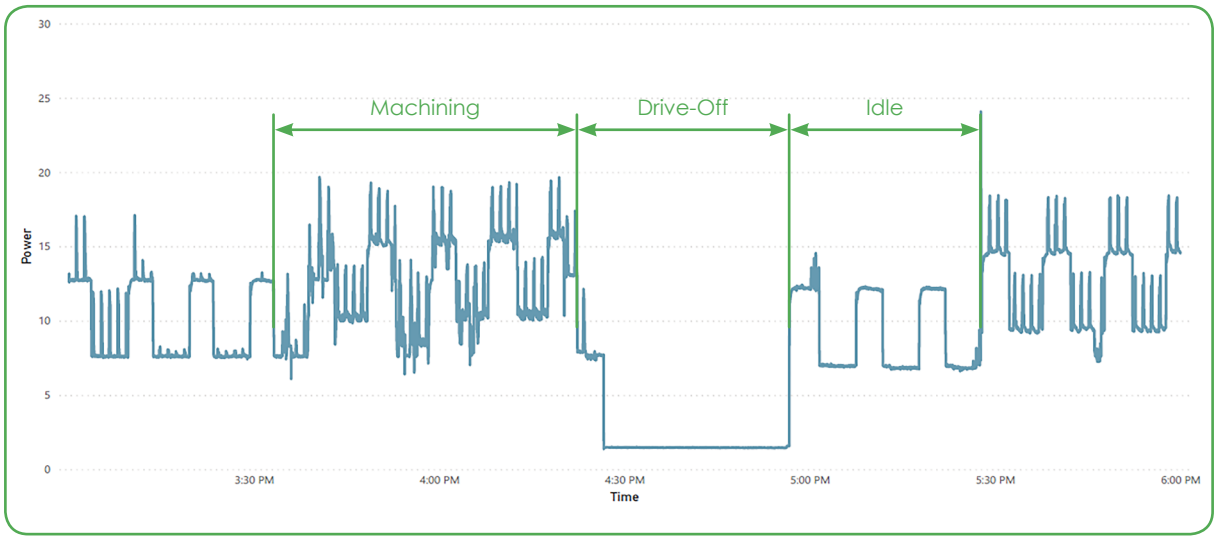

Figure 7 - Comparison of Machining, Idle, and Drive-Off states

■ Modelling of the consumption

To develop an energy consumption estimation model, regression analysis was used to investigate the correlation between total energy usage and the machine's active operating time. Figure 5 shows that the expected consumption nearly matched the actual value, proving the relative accuracy of the regression model. The few existing deviations were typically due to abnormal conditions in the production process such as abnormal chiller performance, incomplete data collection, and issues with auxiliary systems that were not accounted for in the prediction model.

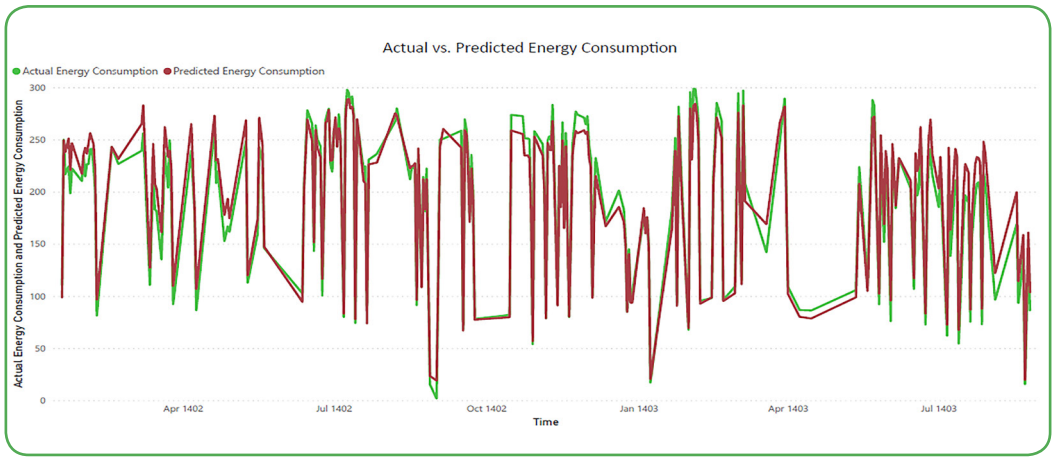

Figure 8 - Performance indicator trend and comparison with the baseline

Results and discussion

According to data analysis and modelling results, among the various factors affecting the machine tool's overall energy consumption, the operation process optimization was the most prominent. Figure 9 illustrates the energy usage patterns before and after the Idle Time Reduction program. There is a significant decrease in energy levels during non-productive machining hours, including quality control stages, workpiece setup, tool change, as well as dinner and lunch break time. The importance of the issue was communicated to machine tool operators via training programs and daily reporting on the machining and idle states. Eventually, continuous monitoring of machine performance and operator training enabled better control of idle time, resulting in less energy waste and increased total production efficiency.

Similar to the machine tool operators, the maintenance staff were also important participants of the idle time reduction program. They were encouraged to participate in this campaign whenever feasible during repair or troubleshooting activities. Table 1 compares two machining instances, identical in temperature and machining time, and different only in idle time. In the first instance, the equipment was deliberately kept in the idle state during maintenance. It is evident that this undue idle time has resulted in a more than twofold increase in energy consumption.

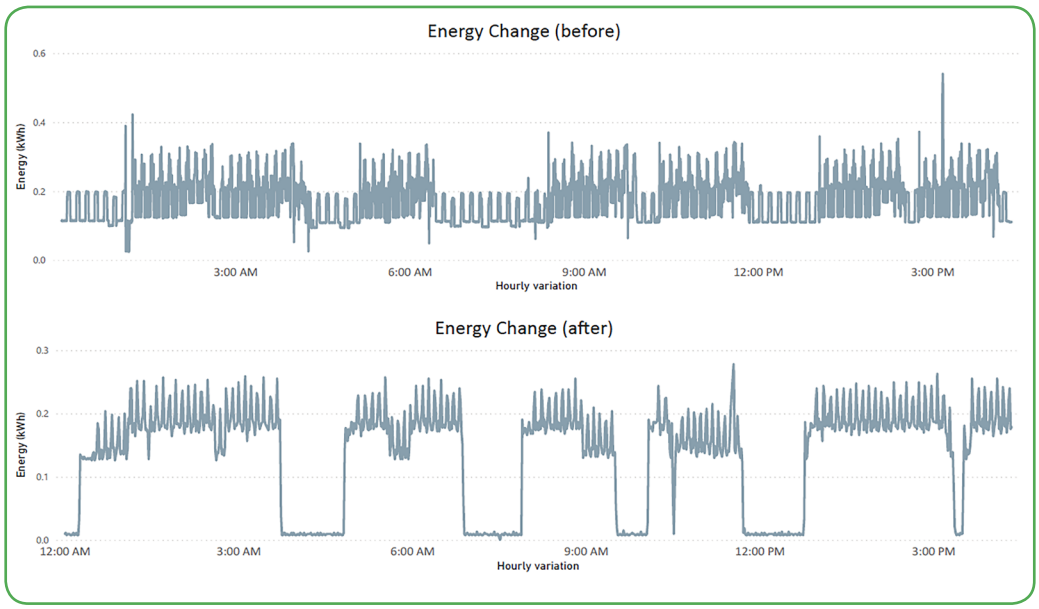

Figure 9 - Energy consumption before and after the Idle Time Reduction program

Table 1 - Case study energy usage, before and after Idle Time Reduction

Date / Period	Temp (°C)	Machining Time (hrs)	Idle Time (hrs)	Actual Energy Consumption (KWh)
2024-05-18	22	6	11	196
2024-11-13	22	6	1	79

This reduction in energy usage becomes more attractive as the program spreads to a greater number of machine tools. Initially, the Idle Time Reduction program targeted only 30% of 4-axis and 5-axis machine tools; after expanding the scope to all corresponding working stations, the factory's overall energy usage decreased by around 7%.

This experience demonstrates the positive impact of continuous monitoring of energy productivity in manufacturing processes. Furthermore, a constant feedback system to foremen of the operation and maintenance teams based on hourly energy usage has been identified to be essential to achieving long-term benefits. It should be noted that less non-productive machining means less stress on the direct drive motion system, which definitely decreases the degradation of mechanical and electrical components.

In addition to the Idle Time Reduction project, additional procedures, such as machine tool auxiliary subsystem contribution to an energy saving program, were discovered to be helpful. Regular Preventive Maintenance (PM) programs and periodic assessments would successfully increase the efficiency of such systems, but with a lesser effect than the Idle Time Reduction scenario.

Concluding Remarks

This study emphasized the importance of energy management in CNC machining operations. Our research began with a data collection effort, then moved on to analytical and modeling tasks, and finally concluded with some practical technological and management recommendations. On a technological level, regular PM plans on auxiliary subsystems were shown to be useful in energy saving plans since CNC machine tools have sophisticated motion control policies that are already energy efficient. At the management level, constant monitoring of inefficient hours combined with operation and maintenance personnel training on energy saving topics were endorsed, which resulted in reduced idle hours, leading to more energy conservation and less machine tool wear. After implementing the related best practices on all corresponding machine tools, a 7% decrease in overall energy usage was achieved. Future efforts will focus on refining these strategies, incorporating more machine specific data, and expanding the scope of energy optimization across additional machinery within the plant.

5

In-Situ Repair of Thermal Barrier Coatings: Extending Service Life Without Downtime

Borghei, Sina

MAPNA Turbine Engineering & Manufacturing Co. (TUGA)

Introduction

The increasing demand for energy efficiency has led researchers across various scientific disciplines to focus on developing products that consume less fuel and energy while offering longer operational lifespans and improved efficiency. This need is particularly crucial for gas turbines and jet engines, which are integral to energy production. Enhancing thermal efficiency of industrial gas turbine engines and aircraft, requires increasing combustion temperatures, but this accelerates the oxidation rates of superalloys, leading to a significant deterioration of their mechanical properties. In response to this challenge, thermal barrier coatings (TBCs) were developed to mitigate the adverse effects of elevated combustion temperatures and enhance turbine efficiency even without the need for disassembly of the hot gas path components, which can significantly reduce downtime and life-cycle costs.

TBC Repair Methods

The concept of employing ceramics as thermal barrier coatings originated in the early 1960s, primarily through initiatives at NASA and the U.S. Air Force Research Center. The typical architecture of thermal barrier coatings, as illustrated in Figure 1, consists of multiple layers: a ceramic top layer, a metallic substrate, and an intermediate metal-based coating (MCrAlY) that serves as an adhesion promoter between the ceramic and the substrate (often a nickel-based superalloy). This intermediate layer not only enhances adhesion, but also protects the substrate from severe oxidation (through thermally grown oxide-TGO layer formation) and improves thermal expansion coefficient compatibility between the ceramic and the underlying metallic substrate.

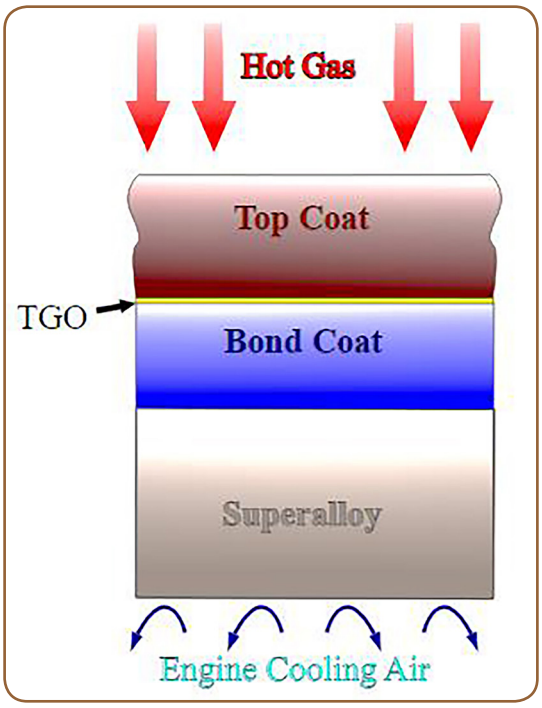

Figure 1 - Schematic of thermal barrier coating

Over the course of service life, thermal barrier coatings degrade, leading to delamination or other local failures which can cause turbine malfunctions, disruptions in energy production, as well as increased operational and maintenance costs. To address these issues, various repair and restoration methods have been developed, categorized as in-situ and off-site measures. Off-site repair methods involve the removal of defective coating, followed by the application of a new one using techniques such as air plasma spraying (APS), high-velocity oxy-fuel (HVOF) spraying, suspension plasma spraying, and vacuum plasma spraying. These methods, while effective, are costly and result in significant downtime in machine operation and energy production.

On the other hand, in-situ repair methods allow for the removal of damaged layers and the application of new coatings without disassembling the components. In-situ techniques include sol-gel processes, immersion, and ceramic pastes application.

Recently, Rolls-Royce has pioneered the use of "SNAKE robot" technology for the in-situ repair of turbine components. In 2009, General Electric Company issued a patent regarding a ceramic paste based on zirconia, binder, and silicone resin. The sintering temperature for this paste was approximately 1000°C. Although this temperature offers more favorable conditions for sintering, it is not applicable in our research, considering working conditions of the target area in gas turbines.

This research aims to synthesize a novel ceramic paste that can be easily applied to surfaces under operational conditions, ideally sintered at approximately 800°C, thereby facilitating repairs during normal operational regimes without extensive downtime.

Experiments

Since the paste synthesized in this research is intended to function similarly to thermal barrier coatings (TBCs), zirconia is identified as the primary component due to its critical role in high-temperature applications. To achieve suitable rheological properties for the paste, it is essential to incorporate solvents and various additives, including binders, plasticizers, dispersants, and antifoaming agents.

A key objective is to reduce the sintering temperature to 800°C without applying external pressure. For this reason, two principal approaches could be employed: 1) the incorporation of zirconia nanoparticles, and 2) the use of sintering aids. Previous studies suggested that combining these approaches yields optimal results, which were adapted, modified, and optimized for this research. Another challenge was synthesizing a silicon-based resin, which serves two functions: 1) enhancing the adhesion of zirconia particles to the substrate and 2) increasing the overall density of the coating by promoting particle adhesion. While the resin formulated by General Electric Co. in its issued patents has become commercially available already, its high sintering temperature and limited availability in global markets, necessitated the synthesis of a suitable alternative.

The initial concept for applying ceramic pastes was derived from existing literature offering the use of a razor and Dr. blade technique. However, its quality is highly reliant on the concentration of the primary components and the production process. Therefore, determining the optimal proportions and synthesis methods for each component is of paramount importance.

Ceramic pastes were applied to prepared (using emery paper mesh No. 400, then acetone cleaning) Inconel 617 samples coated with MCrAlY and subsequently subjected to a series of evaluations following drying and sintering.

■ Rheology

Rheology, the science of material qualities under applied stress, is crucial for understanding the behavior of the paste during application. Since the paste is supposed to be utilized in the Dr. blade method, its rheological properties are fundamental. The rheological characteristics determine the paste's ability to flow beneath the razor and the force required for this flow. The viscosity of the paste was measured as a function of shear rate at 25°C using a PP25 spindle with a rheometer (MCR302, Anton Paar, Austria). The storage modulus (G') and loss modulus (G'') were evaluated through rheological fluctuation tests. The former reflects the elastic properties of the paste; a higher value indicates that the paste behaves more like a solid. Conversely, the loss modulus represents the fluid characteristics of the paste, with an increase indicating a more fluid-like behavior. For effective application using the Dr. blade method, the paste performance lies between solid and fluid states, allowing it to maintain its shape in the absence of applied force while becoming formable under pressure.

■ Adhesion

Adhesion strength of the coatings was evaluated in accordance with ASTM C633 standards. Samples were first cleaned using acetone and subjected to ultrasonic treatment for 5 min. Subsequently, UHU-ENFEST 300 epoxy adhesive was applied to the surfaces. To achieve optimal adhesive strength, the adhesive should be cured at room temperature for 5 min, followed by a further 3 min at room temperature and 3 min at 120°C, until the adhesive strength reaches 15 MPa. Adhesion testing was conducted using an Instron tensile testing machine at a rate of 0.1 cm/s.

■ Hot corrosion

To assess the performance of the coatings under high-temperature conditions, a hot corrosion test was conducted at 860°C using a saturated solution of Na_2SO_4 and 20 wt.% $NaVO_3$. After measuring and weighing the samples, they were preheated to 150°C, and the salt solution was applied using a spraying method. This process allowed for the evaporation of water, resulting in the formation of a thin salt layer on the surface. The Type I hot corrosion test was performed at 860°C for 10 hours, followed by slow cooling of the samples in the furnace. The melting point of the salt composition used is 834°C, and the test was carried out at 860°C to ensure complete melting of the salt and the occurrence of Type I hot corrosion. Weight changes of the samples

were measured at the end of heating and subsequent cooling, which was repeated for a total duration of 100 hours.

Results and discussions

■ Rheology

Figure 2 depicts the curves for both the storage modulus (G') and loss modulus (G'') of this paste.

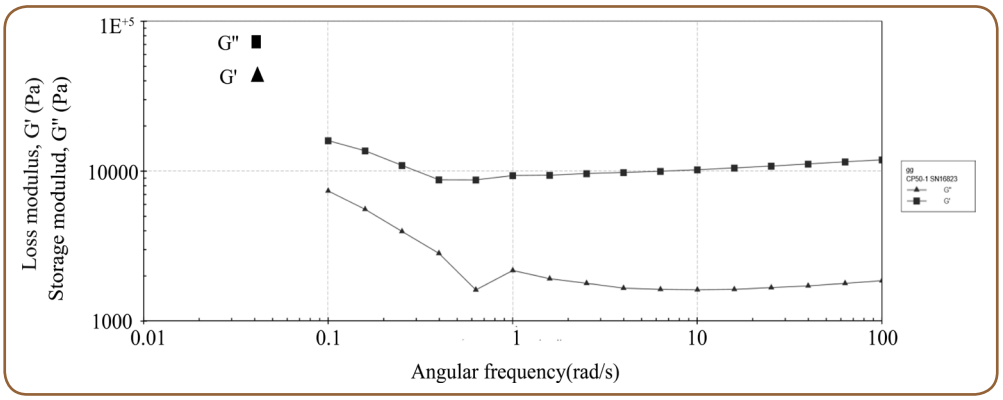

Figure 2 - Alteration of elastic modulus values with respect to angular frequency

The data reveal that across the entire frequency range, the storage modulus consistently exceeds the loss modulus. This observation indicates that the elastic properties of the paste dominate over its viscous characteristics, which is a desirable behavior for materials used in Dr. blade application method. Such a profile ensures that the paste can effectively maintain its structural integrity while also allowing for appropriate flow during application.

■ Adhesion

The results of adhesion strength for the ceramic paste at different sintering temperatures were compared with those of conventional YSZ in thermal barrier coatings (TBCs), as illustrated in Figure 3.

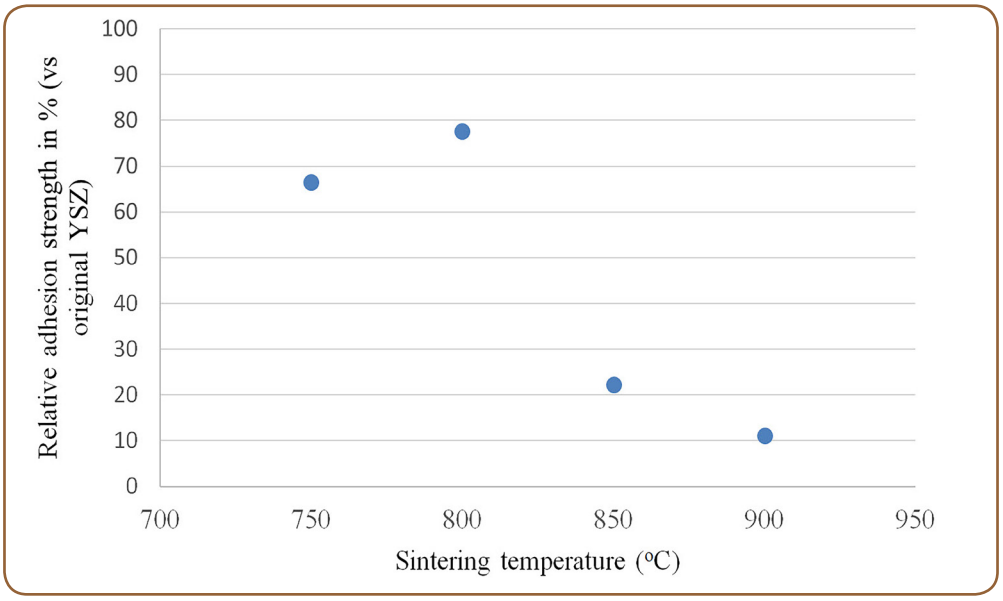

Figure 3 - Adhesion strength of the synthetic ceramic paste

Notably, coatings sintered at temperatures exceeding 850°C often exhibit inadequate adhesion, resulting in delamination. This phenomenon can be attributed to the liquefying of the sintering aid within the coating at elevated temperatures. While this liquid phase facilitates the sintering process and provides the possibility of coating thickness enhancement, it can compromise adhesion at higher temperatures.

The incorporation of silicone resin significantly enhances the adhesion properties of the coating. However, it is critical to optimize the amount of silicone resin used; excessive quantities can introduce oil into the paste, diminishing its necessary brittleness and hindering effective coating application. Furthermore, extending the sintering time does not notably improve coating properties; rather, treatment at temperatures above the optimal level tends to induce cracking within the coatings.

Figure 4 represents electron microscope images of the coating after sintering at 800°C in two magnifications. The image reveals a high-density coating with visible grain indentation, emphasizing the presence of the sintering aid. Additionally, the surface exhibits a minimal number of pores, indicating effective densification.

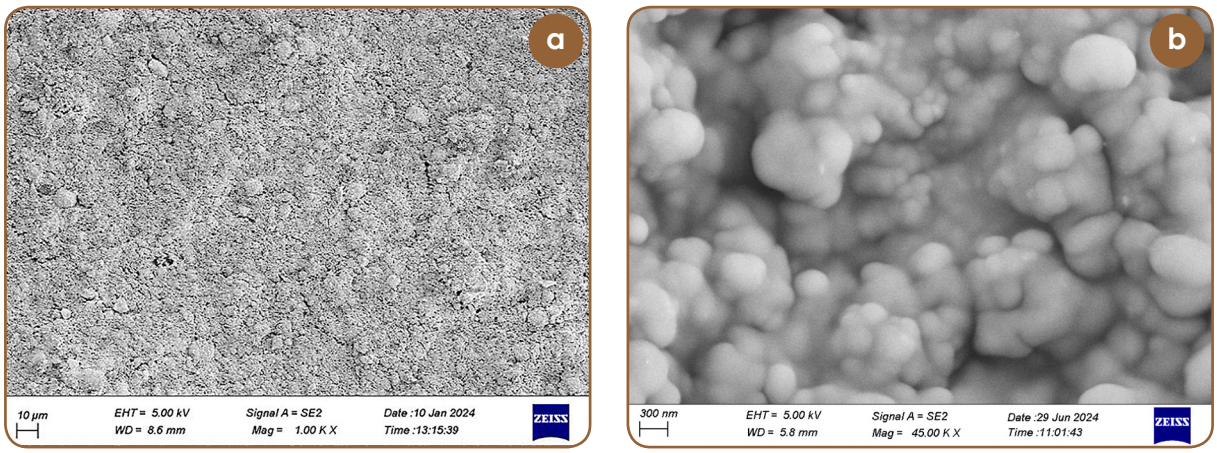

Figure 4 - Microstructure of the ceramic paste at a- 1K and b- 45K magnifications

■ Hot corrosion

The graph illustrating the changes in weight of the sintered sample at a temperature of 800°C is shown in Figure 5.

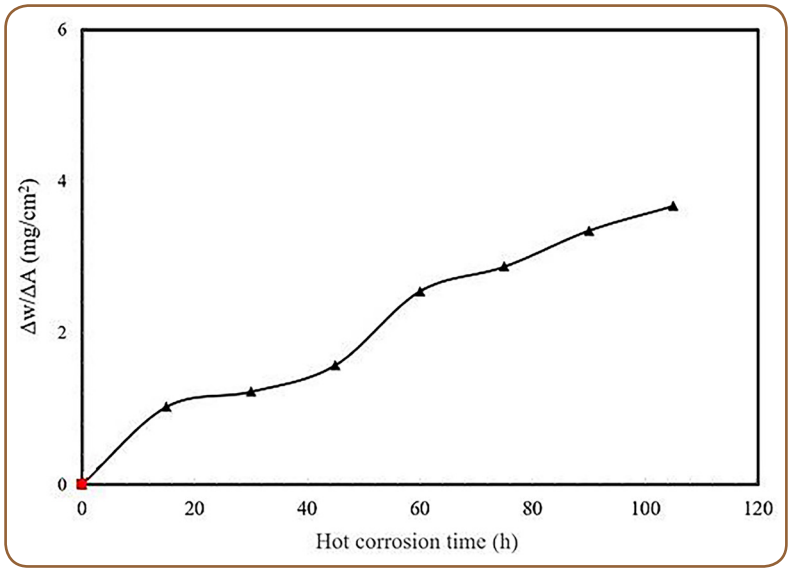

Figure 5 - Weight gain of the synthetic ceramic paste during hot corrosion test

An examination of the physical characteristics of this paste reveals that, after 100 hours of exposure to hot corrosion, oxidation remains the dominant phenomenon. Notably, the flaking of the ceramic coating and oxide layers occurs at a slower rate than that of oxidation. The overall trend depicted in the graph confirms the coatings' commendable resistance to hot corrosion. Importantly, severe flaking was not observed in the samples after 100 hours, and the fluctuations in weight can be attributed to localized flaking in uncovered areas.

After 100 hours of hot corrosion, only minimal signs of peeling were observed, limited to a few isolated spots on the surface. A comparative analysis of the weight change curve and the surface morphology of the samples indicates that these coatings exhibit robust resistance to corrosive environments, as no significant damage was detected according to established criteria.

Figure 6 displays the results of X-ray diffraction analysis conducted on the synthetic ceramic paste in as coated and sintered at 800°C conditions after 100 hours of hot corrosion.

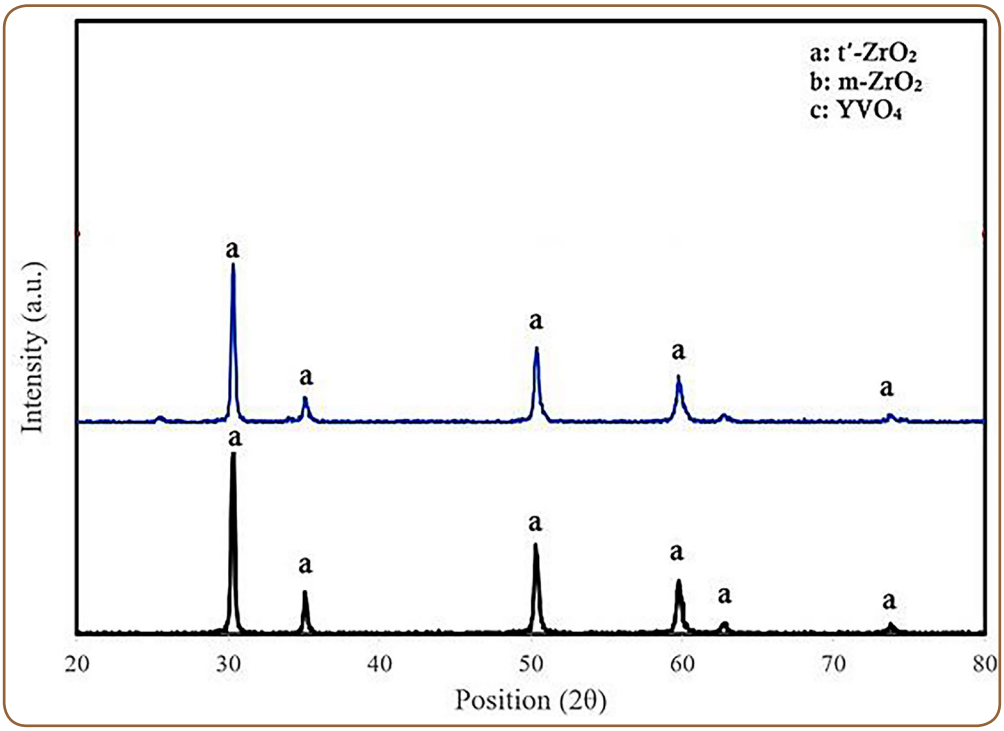

Figure 6 - X-ray diffractometery of bottom; as coated and top; after 100 h hot corrosion tests

The analysis reveals that the stable tetragonal phase (t'-ZrO_2) constitutes the primary phase of the coating. Additionally, after 100 hours of exposure to hot corrosion, both m-ZrO_2 and YVO_4 phases are observed as secondary phases with relatively weak peak intensities. The formation of these secondary phases suggests that destructive reactions have occurred, leading to the leaching of yttrium oxide from the stable zirconia network. The most significant degradation mechanisms in thermal barrier coatings (TBCs) include yttria depletion and zirconia destabilization. Destabilized zirconia can lead to cracking and failure of TBCs during thermal cycling due to volume changes.

To assess the hot corrosion behavior of the ceramic paste synthesized in this research relative to conventional TBC coatings, Figure 7 shows X-ray diffraction analysis results for TBC coatings applied via the atmospheric plasma spraying (APS) method before and after exposure to hot corrosion.

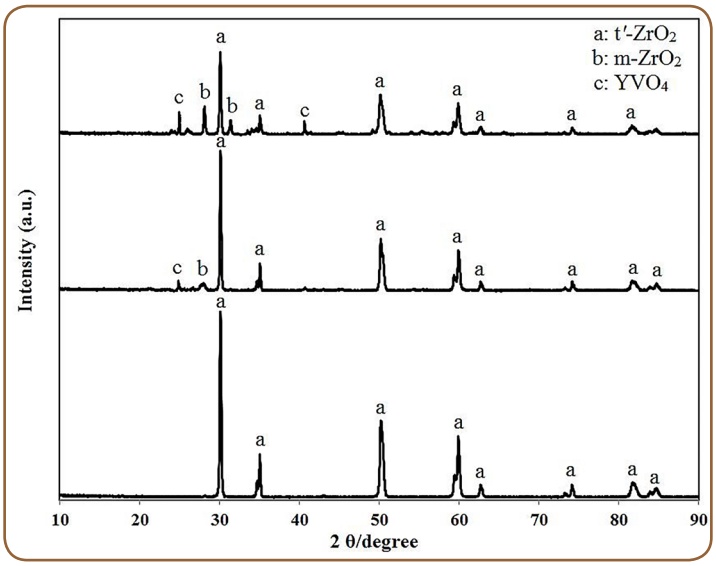

Figure 7 - X-ray diffractometry of bottom; APS coated of conventional TBC, middle; the paste after 60 h, and top; the paste after 100 h hot corrosion tests

It indicates that both coating methods yield similar phase compositions, with both containing a stabilized zirconia phase characterized by a tetragonal structure. However, following hot corrosion exposure, a reduction in tetragonal phase stability is observed in both types of coatings, accompanied by the formation of m-ZrO_2 and YVO_4 phases.

A comparison of phase analysis results after 100 hours of hot corrosion of conventional TBC and the ceramic paste, as shown in Figures 8 and 9, respectively, reveals that peak intensities associated with these secondary phases are higher in TBC coatings produced by the APS method.

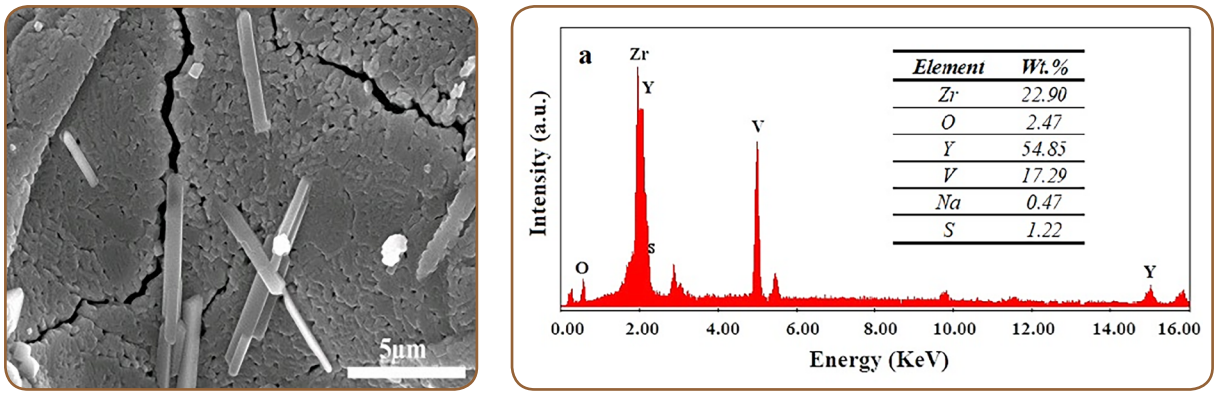

Figure 8 - Elemental analysis on the surface of the conventional TBC after 100 h hot corrosion

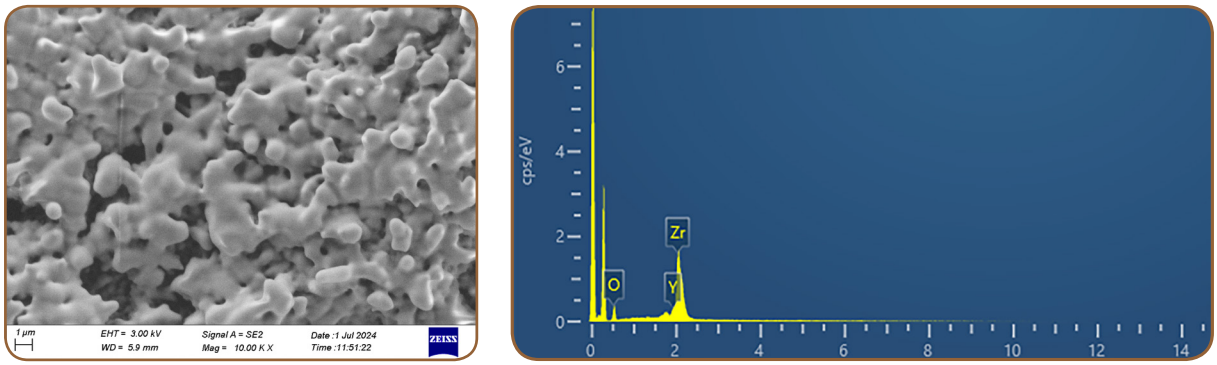

Figure 9 - Elemental analysis on the surface of the ceramic paste after 100 h hot corrosion

This observation can be attributed to the higher density of coatings achieved through that method. Furthermore, due to elevated thermal stresses during thermal spraying processes, coatings produced via APS exhibit a greater number of surface cracks compared to those synthesized in this research. These cracks may facilitate the ingress of corrosive species into the coating, thereby accelerating tetragonal phase decomposition reactions.

Concluding Remarks

In this research, a novel ceramic paste synthesized at TUGA, aiming to facilitate repairs during normal operational regimes without extensive downtime, was studied. This paste can be used to produce repair coatings with thicknesses ranging from 50 to 200 microns and the rheological behavior of the synthetic paste is suitable for application via Dr. blade and spatula techniques.

Comparisons made between the coatings created using this paste and the normal TBC coatings reveal that the synthetic paste sintered at a temperature of 800 °C exhibits the acceptable adhesion strength of 9 MPa (80% of conventional YSZ). Furthermore, the evaluation of the hot corrosion resistance of the repair coating shows that after 100 hours of exposure to corrosive salts, both tetragonal phase stability and surface crack propagation remain minimal compared to initial TBC conditions.

References

[1] M. Aghasibeig, F. Tarasi, R. S. Lima, A. Dolatabadi, and C. Moreau, *"A review on suspension thermal spray patented technology evolution,"* J. Therm. Spray Technol., vol. 28, pp. 1579–1605, 2019.

[2] V. Viswanathan, G. Dwivedi, and S. Sampath, *"Engineered multilayer thermal barrier coatings for enhanced durability and functional performance,"* J. Am. Ceram. Soc., vol. 97, no. 9, pp. 2770–2778, 2014.

[3] X. Yang, J. J. Zhang, Z. Lu, H.-Y. Park, Y.-G. Jung, D. D. Koo, R. Sinatra, and J. J. Zhang, *"Removal and repair techniques for thermal barrier coatings: a review,"* Trans. IMF, vol. 98, no. 3, pp. 121–128, 2020.

MAPNA GROUP
MAPNA Turbine Engineering
and Manufacturing Company

Head Office:
231 Mirdamad Ave. Tehran, I.R.Iran.
P.O.Box: 15875-5643
Tel: +98 (21) 22908581
Fax: +98 (21) 22908654

Factory:
Mapna blvd., Fardis, Karaj, I.R.Iran.
Post code: 31676-43594
Tel: +98 (26) 36630010
Fax: +98 (26) 36612734

www.mapnaturbine.com

tr@mapnaturbine.com

Your opinion matters to us

The technical and other data contained in this Technical Review is provided for information only and may not apply in all cases.

GR686-0